

IUAC School on Nuclear Reactions: The CDCC and CRC methods

Antonio M. Moro



Universidad de Sevilla, Spain

November 15th-20th, 2021

Material available at: <https://github.com/ammoro/IUAC>



Course outline I

1 The CDCC method

- Reminder of the coupled-channels method
- Single-particle and cluster excitations
- Partial wave analysis: radial equations
- Some examples of applications of the CDCC method
- Exploring the continuum with breakup reactions
- Radiative capture from Coulomb dissociation data

2 Advanced CDCC and extensions

- Extension to 3-body projectiles
- Core excitations

3 Application of CDCC to transfer reactions

- Transfer reactions with weakly bound nuclei
- Transfer populating unbound states

4 The Coupled-Reaction Channels (CRC) formalism

5 The problem inclusive breakup

6 Non-elastic breakup

7 The IAV model

- Comparison with inclusive breakup data

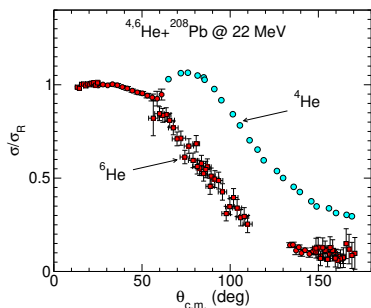
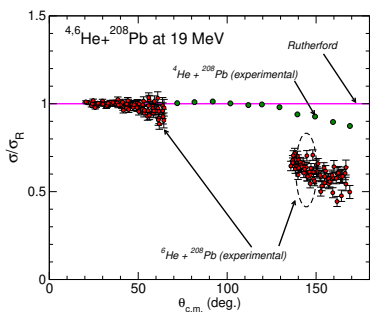
Course outline II

- Applications of the IAV model to fusion



Motivation of the CDCC method

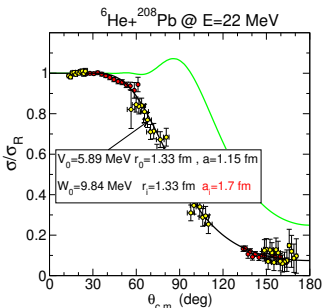
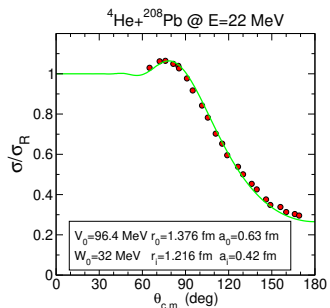
How does the halo structure affect the elastic scattering?



- For $E = 19$ MeV (below the barrier, $V_b \approx 21$ MeV) ^4He follows Rutherford formula.
- ^6He drastically departs from Rutherford formula at both energies!

Motivation of the CDCC method

How does the halo structure affect the elastic scattering?



- ⇒ ${}^4\text{He} + {}^{208}\text{Pb}$ shows typical Fresnel pattern and “standard” optical model parameters
 - ⇒ ${}^6\text{He} + {}^{208}\text{Pb}$ shows a prominent reduction in the elastic cross section, suggesting that part of the incident flux goes to nonelastic channels (e.g. breakup, transfer...)
 - ☞ Understanding and disentangling these nonelastic channels requires going beyond the optical model (eg. [coupled-channels method](#))

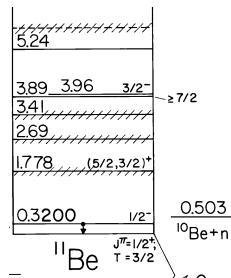
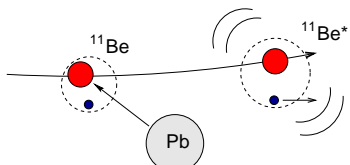


Reminder of the coupled-channels method



Inelastic scattering

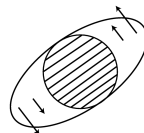
- ⇒ Nuclei are not inert or *frozen* objects; they do have an internal structure of protons and neutrons that can be modified (excited) during the collision.
- ⇒ Quantum systems exhibit, in general, an energy spectrum with bound and unbound levels.



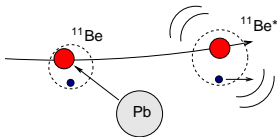


Models for inelastic excitations

- ④ **COLLECTIVE:** Involve a collective motion of several nucleons which can be interpreted macroscopically as **rotations** or **surface vibrations** of the nucleus.



- ④ **FEW-BODY/SINGLE-PARTICLE:** Involve the excitation of a nucleon or cluster.





The coupled-channels method for inelastic scattering

We need to incorporate explicitly in the Hamiltonian the internal structure of the nucleus being excited (e.g. projectile).

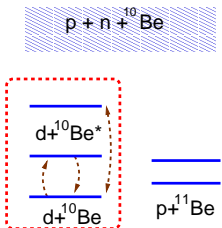
$$H = T_R + h(\xi) + V(\mathbf{R}, \xi)$$

- ⇒ T_R : Kinetic energy for projectile-target relative motion.
 - ⇒ $\{\xi\}$: Internal degrees of freedom of the projectile (depend on the model).
 - ⇒ $V(\mathbf{R}, \xi)$: Projectile-target interaction.
 - ⇒ $h(\xi)$: Internal Hamiltonian of the projectile.

$$h(\xi)\phi_n(\xi) = \varepsilon_n\phi_n(\xi)$$

- ⇒ $\phi_n(\xi)$: internal states of the projectile.

Modelscape and scattering wavefunction: $d + {}^{10}\text{Be} \rightarrow d + {}^{10}\text{Be}^*$ example



- ☞ The modelspace is composed by ground states (elastic channel) and some excited states (inelastic scattering)

Boundary conditions for scattering wavefunction:

$$\Psi_{\mathbf{K}_0}^{(+)}(\mathbf{R}, \xi) \xrightarrow{R \gg} e^{i\mathbf{K}_0 \cdot \mathbf{R}} \phi_0(\xi) + \underbrace{\color{red}f_{0,0}(\theta)}_{\text{incident}} \frac{e^{iK_0 R}}{R} \phi_0(\xi) + \underbrace{\sum_{n>0} \color{red}f_{n,0}(\theta)}_{\text{elastic}} \frac{e^{iK_n R}}{R} \phi_n(\xi)$$

Cross sections:

$$\left(\frac{d\sigma(\theta)}{d\Omega} \right)_{0 \rightarrow n} = \frac{K_n}{K_0} |f_{n,0}(\theta)|^2 \quad f_{n,0}(\theta) = \text{scattering amplitude}$$



CC model wavefunction (target excitation)

We expand the total wave function in a subset of internal states representing the adopted modelspace:

$$\Psi_{\text{model}}(\mathbf{R}, \xi) = \phi_0(\xi)\chi_0(\mathbf{K}_0, \mathbf{R}) + \sum_{n \geq 1} \phi_n(\xi)\chi_n(\mathbf{K}_n, \mathbf{R})$$

and impose the boundary conditions for the (unknown) $\chi_n(\mathbf{R})$:

$$\chi_0^{(+)}(\mathbf{K}_0, \mathbf{R}) \rightarrow e^{i\mathbf{K}_0 \cdot \mathbf{R}} + \cancel{f_{0,0}(\theta)} \frac{e^{iK_0 R}}{R} \quad \text{for n=0 (elastic)}$$

$$\chi_n^{(+)}(\mathbf{K}_n, \mathbf{R}) \rightarrow \cancel{f_{n,0}(\theta)} \frac{e^{iK_n R}}{R} \quad \text{for n>0 (non-elastic)}$$



Calculation of $\chi_n^{(+)}(\mathbf{R})$: the coupled equations

- ⇒ The model wavefunction must satisfy the Schrödinger equation:

$$[H - E]\Psi_{\text{model}}^{(+)}(\mathbf{R}, \xi) = 0$$

- ⇒ Multiply on the left by each $\phi_n^*(\xi)$, and integrate over $\xi \Rightarrow$ coupled channels equations for $\{\chi_n(\mathbf{R})\}$:

$$[E - \varepsilon_n - T_R - V_{n,n}(\mathbf{R})]\chi_n(\mathbf{R}) = \sum_{n' \neq n} V_{n,n'}(\mathbf{R})\chi_{n'}(\mathbf{R})$$

- ⇒ The structure information is embedded in the coupling potentials:

$$V_{n,n'}(\mathbf{R}) = \int d\xi \phi_{n'}^*(\xi) V(\mathbf{R}, \xi) \phi_n(\xi)$$

☞ $\phi_n(\xi)$ will depend on the assumed structure model (collective, few-body, etc).

oo

Optical Model vs. Coupled-Channels method

Optical Model

- ### ⇒ The Hamiltonian:

$$H = T_R + V(\mathbf{R})$$

- ⇒ Internal states: Just $\phi_0(\xi)$

- ### ⇒ Model wavefunction:

$$\Psi_{\text{mod}}(\mathbf{R}, \xi) \equiv \chi_0(\mathbf{K}, \mathbf{R}) \phi_0(\xi)$$

- ### ⇒ Schrödinger equation:

$$[H - E]\chi_0(\mathbf{K}, \mathbf{R}) = 0$$

Optical Model vs. Coupled-Channels method

Optical Model

- ⇒ The Hamiltonian:

$$H = T_R + V(\mathbf{R})$$
 - ⇒ Internal states: Just $\phi_0(\xi)$
 - ⇒ Model wavefunction:

$$\Psi_{\text{mod}}(\mathbf{R}, \xi) \equiv \chi_0(\mathbf{K}, \mathbf{R})\phi_0(\xi)$$
 - ⇒ Schrödinger equation:

$$[H - E]\chi_0(\mathbf{K}, \mathbf{R}) = 0$$

Coupled-channels method

- ⇒ The Hamiltonian:

$$H = T_R + h(\xi) + V(\mathbf{R}, \xi)$$
 - ⇒ Internal states:

$$h(\xi)\phi_n(\xi) = \varepsilon_n\phi_n(\xi)$$
 - ⇒ Model wavefunction:

$$\Psi_{\text{model}}(\mathbf{R}, \xi) = \phi_0(\xi)\chi_0(\mathbf{K}, \mathbf{R}) + \sum_{n>0} \phi_n(\xi)\chi_n(\mathbf{K}, \mathbf{R})$$
 - ⇒ Schrödinger equation:

$$[H - E]\Psi_{\text{model}}(\mathbf{R}, \xi) = 0$$

↓

$$[E - \varepsilon_n - T_R - V_{n,n}(\mathbf{R})] \chi_n(\mathbf{K}, \mathbf{R}) = \sum_{n' \neq n} V_{n,n'}(\mathbf{R}) \chi_{n'}(\mathbf{K}, \mathbf{R})$$

DWBA approximation as 1st order CC

- Two-states model $n \equiv 0, 1$:

$$\Psi(\mathbf{R}, \xi) = \underbrace{\phi_0(\xi)\chi_0(\mathbf{R})}_{\text{elastic}} + \underbrace{\phi_1(\xi)\chi_1(\mathbf{R})}_{\text{inelastic}}$$

- ### ⇒ Coupled-channels equations:

$$[E - \varepsilon_0 - T_0 - V_{00}(\mathbf{R})] \chi_0(\mathbf{R}) = V_{01}(\mathbf{R}) \chi_1(\mathbf{R})$$

$$[E - \varepsilon_1 - T_1 - V_{11}(\mathbf{R})] \chi_1(\mathbf{R}) = V_{10}(\mathbf{R}) \chi_0(\mathbf{R})$$

- ⇒ Iterative solution of the CC equations (DWBA):

$$[E - \varepsilon_0 - T_0 - V_{00}(\mathbf{R})] \chi_0(\mathbf{R}) \approx 0$$

$$[E - \varepsilon_1 - T_1 - V_{11}(\mathbf{R})] \chi_1(\mathbf{R}) \approx V_{10}(\mathbf{R}) \chi_0(\mathbf{R})$$

DWBA approximation as 1st order CC

⇒ Asymptotically:

$$\chi_1^{(+)}(\mathbf{R}) \rightarrow f_{10}(\theta) \frac{e^{iK_1 R}}{R}$$

with (not proven here!)

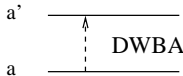
$$f_{10}(\theta) = -\frac{2\mu}{4\pi\hbar^2} \int d\mathbf{R} \tilde{\chi}_1^{(-)*}(\mathbf{K}_1, \mathbf{R}) V_{10}(\mathbf{R}) \tilde{\chi}_0^{(+)}(\mathbf{K}_0, \mathbf{R})$$

where $\tilde{\chi}_0(\mathbf{K}_0, \mathbf{R}), \tilde{\chi}_1(\mathbf{K}_1, \mathbf{R})$ are solutions of:

$$[E - \varepsilon_0 - T_0 - V_{00}(\mathbf{R})]\tilde{\chi}_0(\mathbf{K}_0, \mathbf{R}) = 0$$

$$[E - \varepsilon_1 - T_1 - V_{11}(\mathbf{R})]\tilde{\chi}_1(\mathbf{K}_1, \mathbf{R}) = 0$$

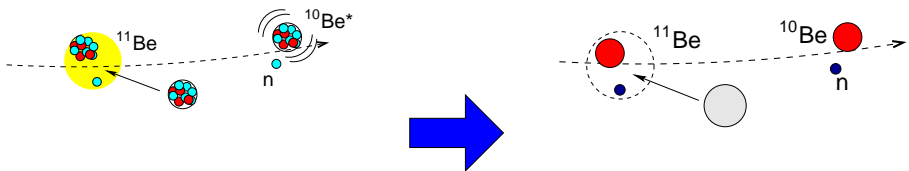
- ☞ The DWBA approximation amounts at solving the CC equations to 1st order (Born approximation)





Single-particle and cluster excitations

Many-body to few-body reduction



$$\mathcal{V}_{pt} = \sum_{ij} V_{ij}(\mathbf{r}_{ij})$$

$$\mathcal{V}_{pt} = U_{ct}(\mathbf{r}_{ct}) + U_{nt}(\mathbf{r}_{nt})$$

⇒ Effective **three-body** Hamiltonian:

$$H = T_{\mathbf{R}} + h_r(\mathbf{r}) + U_{ct}(\mathbf{r}_{ct}) + U_{nt}(\mathbf{r}_{nt})$$

⇒ $U_{ct}(\mathbf{r}_{ct})$, $U_{nt}(\mathbf{r}_{nt})$ are optical potentials describing fragment-target elastic scattering (eg. target excitation is treated effectively, through absorption)



Inelastic scattering in a few-body model

- ⇒ Some nuclei allow a description in terms of two or more clusters:
 $d=p+n$, ${}^6\text{Li}=\alpha+d$, ${}^7\text{Li}=\alpha+{}^3\text{H}$.
- ⇒ Projectile-target interaction:

$$V(\mathbf{R}, \xi) \equiv V(\mathbf{R}, \mathbf{r}) = U_1(\mathbf{r}_1) + U_2(\mathbf{r}_2)$$

- ⇒ Transition potentials:

$$V_{n,n'}(\mathbf{R}) = \int d\mathbf{r} \phi_n^*(\mathbf{r}) [U_1(\mathbf{r}_1) + U_2(\mathbf{r}_2)] \phi_{n'}(\mathbf{r})$$



Inelastic scattering in a few-body model

- ⇒ Some nuclei allow a description in terms of two or more clusters:
 $d=p+n$, ${}^6\text{Li}=\alpha+d$, ${}^7\text{Li}=\alpha+{}^3\text{H}$.
- ⇒ Projectile-target interaction:

$$V(\mathbf{R}, \xi) \equiv V(\mathbf{R}, \mathbf{r}) = U_1(\mathbf{r}_1) + U_2(\mathbf{r}_2)$$

- ⇒ Transition potentials:

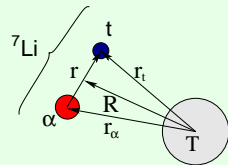
$$V_{n,n'}(\mathbf{R}) = \int d\mathbf{r} \phi_n^*(\mathbf{r}) [U_1(\mathbf{r}_1) + U_2(\mathbf{r}_2)] \phi_{n'}(\mathbf{r})$$

Example: ${}^7\text{Li}=\alpha+t$

$$\mathbf{r}_\alpha = \mathbf{R} - \frac{m_t}{m_\alpha + m_t} \mathbf{r}; \quad \mathbf{r}_t = \mathbf{R} + \frac{m_\alpha}{m_\alpha + m_t} \mathbf{r}$$

Internal states: (two-body cluster model)

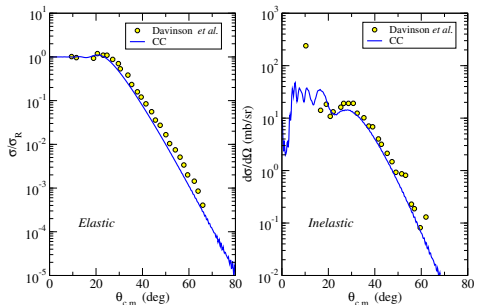
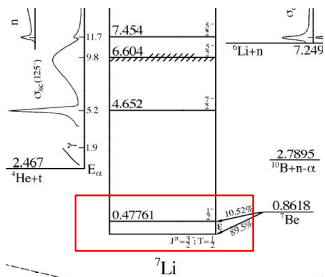
$$[T_{\mathbf{r}} + V_{\alpha-t}(\mathbf{r}) - \varepsilon_n] \phi_n(\mathbf{r}) = 0$$





Example: ${}^7\text{Li}(\alpha+t) + {}^{208}\text{Pb}$ at 68 MeV

⇒ CC calculation with 2 channels ($3/2^-$, $1/2^-$):



Data from Davinson et al, Phys. Lett. 139B (1984) 150

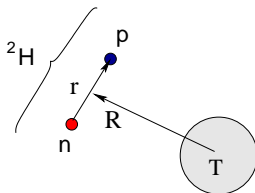
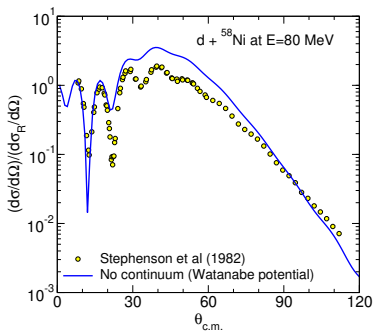
Fresco input available at <https://github.com/ammoro/IUAC>



Application of the CC method to weakly-bound systems

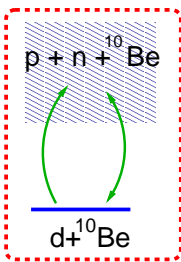
Example: Three-body calculation ($p + n + {}^{58}\text{Ni}$) with Watanabe potential:

$$V_{dt}(\mathbf{R}) = \int d\mathbf{r} \phi_{gs}^*(\mathbf{r}) \left\{ V_{pt}(\mathbf{r}_{pt}) + V_{nt}(\mathbf{r}_{nt}) \right\} \phi_{gs}(\mathbf{r})$$



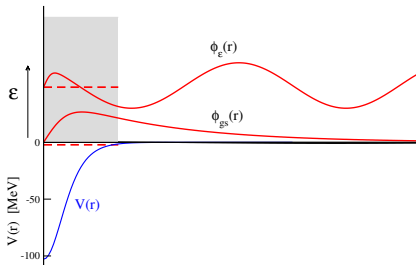
☞ Three-body calculations omitting breakup channels fail to describe the experimental data.

Extension of the CC to unbound states



We want to include explicitly in the modelspace the breakup channels of the projectile or target.

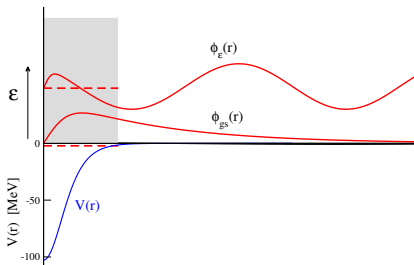
Bound versus scattering states



Continuum wavefunctions:

$$\varphi_{k,\ell jm}(\mathbf{r}) = \frac{u_{k,\ell j}(r)}{r} [Y_\ell(\hat{r}) \otimes \chi_s]_{jm}$$

Bound versus scattering states



Continuum wavefunctions:

$$\varphi_{k,\ell jm}(\mathbf{r}) = \frac{u_{k,\ell j}(r)}{r} [Y_\ell(\hat{r}) \otimes \chi_s]_{jm}$$

Unbound states are not suitable for CC calculations:

- They have a continuous (infinite) distribution in energy.
 - Non-normalizable: $\langle u_{k,\ell,si}(r)|u_{k',\ell,si}(r)\rangle \propto \delta(k - k')$

SOLUTION \Rightarrow continuum discretization



The origins of CDCC

- ⇒ Continuum discretization method proposed by G.H. Rawitscher [PRC9, 2210 (1974)] and Farrell, Vincent and Austern [Ann.Phys.(New York) 96, 333 (1976)] to describe deuteron scattering as an effective three-body problem $p + n + A$.

PHYSICAL REVIEW C

VOLUME 9, NUMBER 6

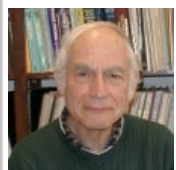
JUNE 1974

Effect of deuteron breakup on elastic deuteron-nucleus scattering

George H. Rawitscher*

*Center for Theoretical Physics, Massachusetts Institute of Technology, Cambridge, Massachusetts 02139,[†]
and Department of Physics, University of Surrey, Guildford, Surrey, England
(Received 1 October 1973; revised manuscript received 4 March 1974)*

The properties of the transition matrix elements $V_{ab}(R)$ of the breakup potential V_N taken between states $\phi_a(\vec{r})$ and $\phi_b(r)$ are examined. Here $\phi_a(\vec{r})$ are eigenstates of the neutron-proton relative-motion Hamiltonian, and the eigenvalues of the energy ϵ_a are positive (continuum states) or negative (bound deuteron); $V_N(\vec{r}, \vec{R})$ is the sum of the phenomenological proton-nucleus $V_{p-A}(\vec{R} - \frac{1}{2}\vec{r})$ and neutron nucleus $V_{n-A}(\vec{R} + \frac{1}{2}\vec{r})$ optical potentials evaluated for nucleon energies equal to half the incident deuteron energy. The bound-to-continuum transition matrix element for relative neutron-proton angular momenta $l=2$ are found to be comparable in magnitude to the ones for $l=0$ for values of ϵ_a larger than about 3 MeV, and both decrease only slowly with ϵ_a , suggesting that a large breakup spectrum is involved in deuteron-nucleus collisions. The effect of the various breakup transitions on the elastic phase shifts is estimated by numerically solving a set of coupled equations. These equations couple the functions $x_a(\vec{R})$ which are the coefficients of the expansion of the neutron-proton-nucleus wave function in a set of the $\phi_b(\vec{r})$'s. The equations are rendered manageable by performing a (rather crude) discretization in the neutron-proton relative-momentum variable k_a . Numer-

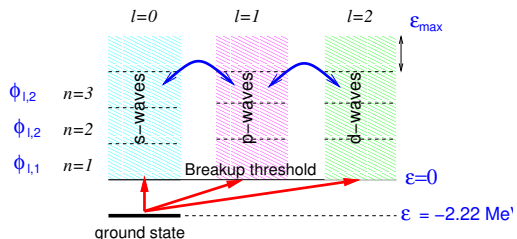


George Rawitscher
(1928-2018)

- ⇒ Full numerical implementation by Kyushu group (Sakuragi, Yahiro, Kamimura, and co.):
Prog. Theor. Phys.(Kyoto) 68, 322 (1982)



Continuum discretization for deuteron scattering



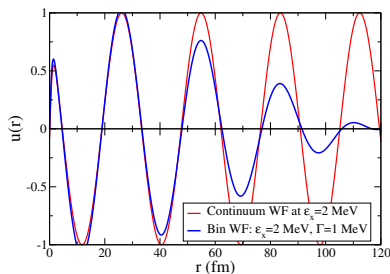
- ⇒ Select a number of angular momenta ($\ell = 0, \dots, \ell_{\max}$).
- ⇒ For each ℓ , set a maximum excitation energy ϵ_{\max} .
- ⇒ Divide the interval $\epsilon = 0 - \epsilon_{\max}$ in a set of sub-intervals (*bins*).
- ⇒ For each *bin*, calculate a representative wavefunction.

Bin wavefunction:

$$\phi_{\ell jm}^{[k_1, k_2]}(\mathbf{r}) = \frac{u_{\ell j}^{[k_1, k_2]}(r)}{r} [Y_\ell(\hat{\mathbf{r}}) \otimes \chi_s]_{jm} \quad [k_1, k_2] = \text{bin interval}$$

$$u_{\ell sjm}^{[k_1, k_2]}(r) = \sqrt{\frac{2}{\pi N}} \int_{k_1}^{k_2} w(k) u_{k, \ell sj}(r) dk$$

- ⇒ k : linear momentum
 - ⇒ $u_{k,\ell s j}(\mathbf{r})$: scattering states (radial part)
 - ⇒ $w(k)$: weight function



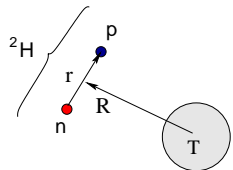


CDCC formalism for deuteron scattering

- ⇒ Hamiltonian: $H = T_{\mathbf{R}} + h_r(\mathbf{r}) + V_{pt}(\mathbf{r}_{pt}) + V_{nt}(\mathbf{r}_{nt})$
- ⇒ Model wavefunction:

$$\Psi^{(+)}(\mathbf{R}, \mathbf{r}) = \phi_{gs}(\mathbf{r})\chi_0(\mathbf{R}) + \sum_{n>0}^N \phi_n(\mathbf{r})\chi_n(\mathbf{R})$$

- ⇒ Coupled equations: $[H - E]\Psi(\mathbf{R}, \mathbf{r}) = 0$



$$[E - \varepsilon_n - T_R - V_{n,n}(\mathbf{R})]\chi_n(\mathbf{R}) = \sum_{n' \neq n} V_{n,n'}(\mathbf{R})\chi_{n'}(\mathbf{R})$$

- ⇒ Transition potentials:

$$V_{n;n'}(\mathbf{R}) = \int d\mathbf{r} \phi_n^*(\mathbf{r}) \left[V_{pt}(\mathbf{R} + \frac{\mathbf{r}}{2}) + V_{nt}(\mathbf{R} - \frac{\mathbf{r}}{2}) \right] \phi_{n'}(\mathbf{r})$$

Partial-wave decomposition of CDCC wavefunction

- In practical calculations, the CDCC wf is expanded in the so-called channel basis

$$\langle \hat{R}, \mathbf{r}, |\beta; J_T \rangle = \left[Y_L(\hat{R}) \otimes \phi_{n, J_p}(\mathbf{r}) \right]_{J_T} :$$

$$\Psi_{\beta_0, J_T, M_T}(\vec{R}, \vec{r}, \xi) = \sum_{\beta} \frac{\chi_{\beta, \beta_0}^{J_T}(R)}{R} |\beta; J_T\rangle \quad \beta \equiv \{L, J_p, n\}$$

- ⇒ The radial coefficients verify

$$\left(-\frac{\hbar^2}{2\mu} \frac{d^2}{dR^2} + \frac{\hbar^2 L(L+1)}{2\mu R^2} + \varepsilon_n - E \right) \chi_{\beta,\beta_0}^{J_T}(R) + \sum_{\beta'} V_{\beta,\beta'}^{J_T}(R) \chi_{\beta'}^{J_T}(R) = 0$$

with the coupling potentials:

$$V_{\beta\beta'}^{J_T}(R) = \langle \beta; J_T | V_1(\vec{R}, \vec{r}) + V_2(\vec{R}, \vec{r}) | \beta'; J_T \rangle$$

- ### → Boundary conditions:

$$\chi_{\beta,\beta_0}^{J_T}(R) \rightarrow e^{i\sigma_L} \frac{i}{2} \left[H_L^{(-)}(K_\beta R) \delta_{\beta_0,\beta} - S_{\beta,\beta_0}^{J_T} H_L^{(+)}(K_\beta R) \right]$$



Trivially equivalent local equivalent potential (TELP)

- From the elastic channel equation, a TELP can be defined as follows:

$$\left[E - \varepsilon_0 - \hat{T}_{\mathbf{R}} - V_{0,0}(\mathbf{R}) \right] \chi_0(\mathbf{R}) = \sum_{i \neq 0} V_{i,0}(\mathbf{R}) \chi_i(\mathbf{R}) \equiv U_{\text{TELP}}(\mathbf{R}) \chi_0(\mathbf{R}).$$

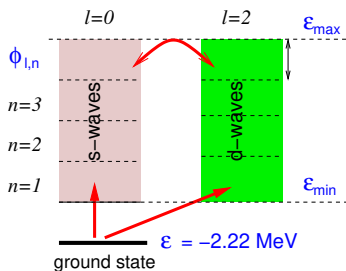
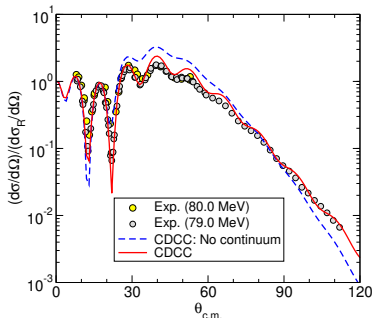
- In actual calculations, $U_{\text{TELP}}(\mathbf{R})$ will depend on the total angular momentum, but a weighted average can be performed to obtain an approximate angular-momentum independent polarization potential
- A single channel calculation with the potential $U(\mathbf{R}) = V_{0,0}(\mathbf{R}) + U_{\text{TELP}}(\mathbf{R})$ should reproduce approximately the elastic scattering cross section.



Applications of the CDCC formalism: d+⁵⁸Ni

Coupling to continuum states produce:

- ⇒ Polarization of the projectile (modification of real part)
- ⇒ Flux removal (absorption) from the elastic channel (imaginary part)

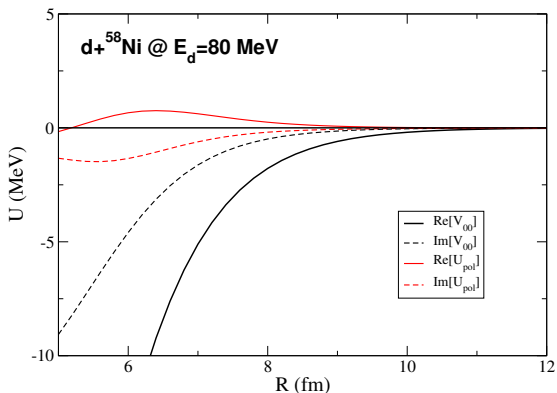


- ⇒ No continuum ⇒ retain only the Watanabe potential:

$$V_{00}(\mathbf{R}) = \int d\mathbf{r} \phi_{gs}(\mathbf{r}) (V_{pt} + V_{nt}) \phi_{gs}(\mathbf{r})$$



Trivially equivalent local equivalent potential for $d+^{58}\text{Ni}$ @ 80 MeV



For this reaction, the TELP is complex:

- ⇒ The real part is **repulsive** (reduces projectile-target attraction)
- ⇒ The imaginary part is **absorptive** (flux removal)



Two- and three-body breakup observables

- CDCC scattering amplitudes readily provide **two-body breakup** observables:

$$\frac{d\sigma_n}{d\Omega_{\text{c.m.}}} = |f_{0,n}(\theta)|^2 \Rightarrow \frac{d^2\sigma}{d\Omega_{\text{c.m.}} d\epsilon_{pn}} \simeq \frac{1}{\Delta_n} \frac{d\sigma_n}{d\Omega_{\text{c.m.}}}$$

with:

- Δ_n =width of the bin containing the relative energy ϵ_{pn}
- $\Omega_{\text{c.m.}}$ =C.M. scattering angle of the projectile c.m. (not easy to measure!)

- Three-body observables** can be also calculated using a suitable combination of the scattering amplitudes and appropriate kinematical transformations ([Tostevin, PRC63, 024617 \(2001\)](#)):

$$\frac{d^3\sigma}{d\Omega_n d\Omega_p dE_p}$$

- N.b.:** These 3-body observables are not directly provided by FRESCO. They must be computed separately from the calculated amplitudes.

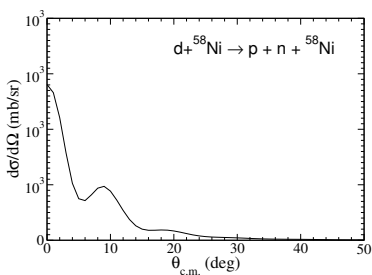


Two-body breakup observables: $d + {}^{58}\text{Ni} \rightarrow p + n + {}^{58}\text{Ni}$

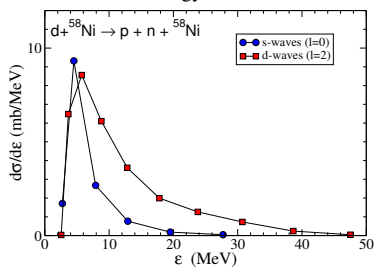
CDCC calculations for $d + {}^{58}\text{Ni}$ at 80 MeV :

- ⇒ Continuum states with $\ell = 0, 2$.
- ⇒ Proton and neutron intrinsic spins ignored.
- ⇒ $p/n + {}^{58}\text{Ni}$ from global optical potential.
- ⇒ $p+n$ simple Gaussian interaction describing deuteron g.s.

$p + n$ c.m. angular distribution



Excitation energy distribution



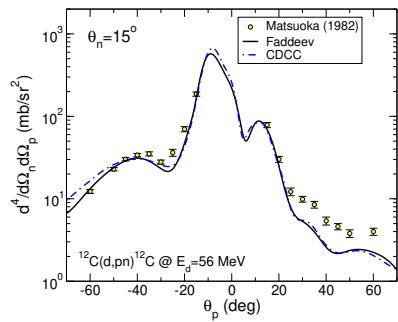
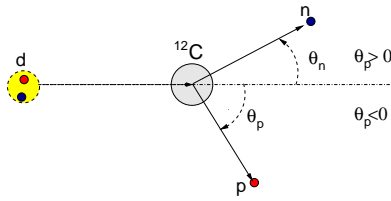


Breakup observables with CDCC: exclusive breakup of $d + {}^{12}\text{C} \rightarrow p + n + {}^{12}\text{C}$

CDCC calculations for $d + {}^{12}\text{C}$ at 56 MeV:

- ⇒ Continuum states with $\ell \leq 8$ and $\varepsilon_{\max} = 46$ MeV.
- ⇒ Proton and neutron intrinsic spins ignored
- ⇒ $p/n + {}^{58}\text{Ni}$ from Watson global optical potential
- ⇒ $p+n$ simple Gaussian interaction describing deuteron g.s.

Data: Matsuoka *et al.*, NPA391, 357 (1982).



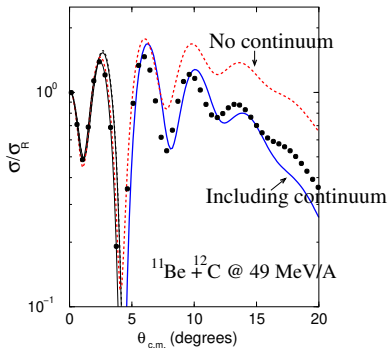
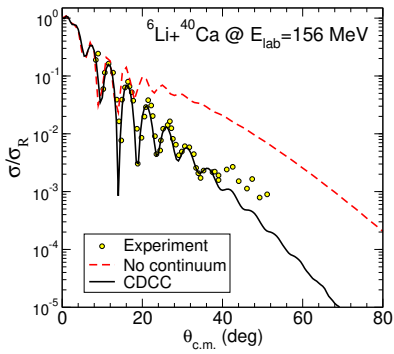
A.Deltuva, A.M.M., E.Cravo, F.M.Nunes, A.C.Fonseca, PRC 76, 064602 (2007)



Application of the CDCC method to other weakly bound two-body nuclei

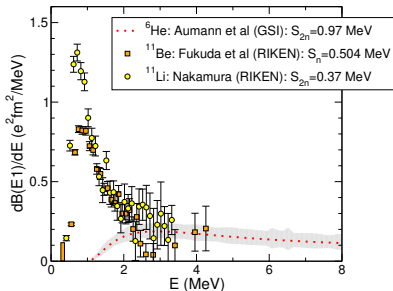
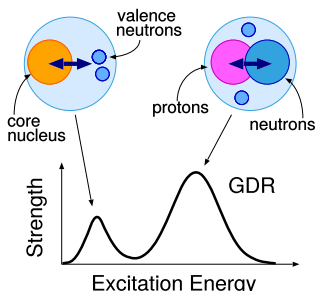
The CDCC has been also applied to nuclei with a cluster structure:

- ⇒ ${}^6\text{Li} = \alpha + \text{d}$ ($S_{\alpha,d} = 1.47 \text{ MeV}$)
- ⇒ ${}^{11}\text{Be} = {}^{10}\text{Be} + \text{n}$ ($S_n = 0.504 \text{ MeV}$)



Exploring the continuum with breakup reactions

Electric response of weakly-bound nuclei



- ⇒ The $E\lambda$ response can be quantified through the $B(E\lambda)$ probability:

$$B(E\lambda; i \rightarrow f) = \frac{1}{2I_i + 1} |\langle \Psi_f | \mathcal{M}(E\lambda) | \Psi_i \rangle|^2$$

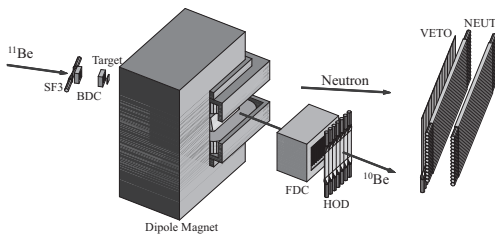
- ⇒ Neutron-halo nuclei have large $B(E1)$ strengths near threshold



How to probe/extract the $B(E1)$ of halo nuclei?

Example: $^{11}\text{Be} + ^{208}\text{Pb} \rightarrow ^{10}\text{Be} + \text{n} + ^{208}\text{Pb}$ measured at RIKEN (69 MeV/u).

Fukuda et al, PRC70, 054606 (2004))



- 11Be excitation energy can be reconstructed from core-neutron coincidences (*invariant mass method*)

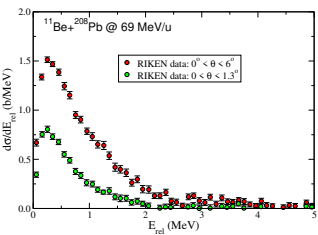
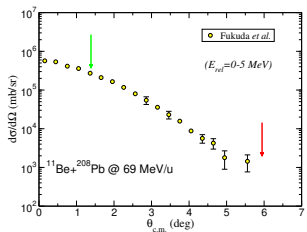


What observables are measured in Coulomb dissociation experiments?

- ⇒ In a fully exclusive experiment, one can in principle measure the angular and relative energy distribution of the $^{11}\text{Be}^*$ system:

$$\frac{d^2\sigma}{d\Omega dE_{\text{rel}}}$$

- ⇒ Integrating over the angle or energy, single differential cross sections are obtained:



- ⇒ In the Coulomb dominated region (i.e. small angles), the **breakup cross section** is expected to be dominated by the $dB(E\lambda)/dE$ distribution, but we need a theory that relates both observables.



Semiclassical 1st order E λ excitation (Alder & Winther) (akin EPM method)

- For E λ excitation to bound states ($0 \rightarrow n$):

$$\left(\frac{d\sigma}{d\Omega} \right)_{0 \rightarrow n} = \left(\frac{Z_t e^2}{\hbar v} \right)^2 \frac{B(E\lambda, 0 \rightarrow n)}{e^2 a_0^{2\lambda-2}} f_\lambda(\theta, \xi)$$

$$\xi_{0 \rightarrow n} = \frac{(E_n - E_0)}{\hbar} \frac{a_0}{v}$$

- For continuum states (breakup):

$$\frac{d\sigma(E\lambda)}{d\Omega dE} = \left(\frac{Z_t e^2}{\hbar v} \right)^2 \frac{1}{e^2 a_0^{2\lambda-2}} \frac{dB(E\lambda)}{dE} \frac{df_\lambda(\theta, \xi)}{d\Omega}$$

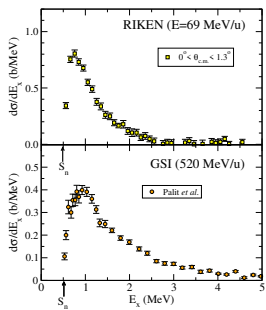
- $dB(E\lambda)/dE$ can be extracted from small-angle Coulomb dissociation data.

$$\frac{d\sigma}{dE}(\theta < \theta_{\max}) = \int_0^{\theta_{\max}} \frac{d\sigma(E\lambda)}{d\Omega dE} d\Omega \propto \frac{dB(E\lambda)}{dE}$$

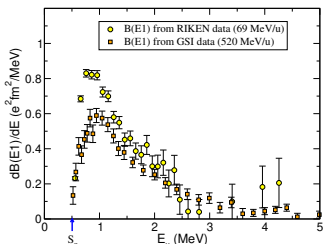
Extracting $B(E1)$ of ^{11}Be from $^{11}\text{Be} + ^{208}\text{Pb}$ Coulomb dissociation

Common assumptions:

- ⇒ Breakup dominated by Coulomb excitation
 - ⇒ Nuclear excitation, if present, can be estimated and added incoherently
 - ☞ If the assumptions above are fulfilled, the extracted $dB(E\lambda)dE$ should be independent of the incident energy and target employed, since it reflects a structure property of the projectile.



$$\frac{dB(E\lambda)}{dE} \propto \frac{d\sigma}{dE}$$



RIKEN: Fukuda et al, PRC70 (2004) 054606
GSI: Palit et al, PRC68 (2003) 034318

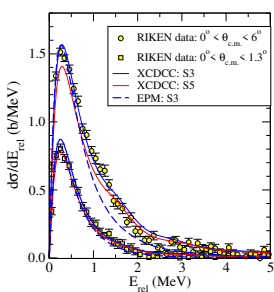
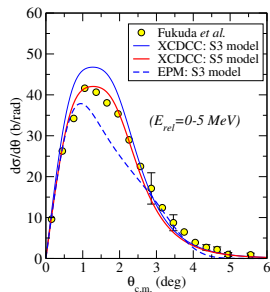
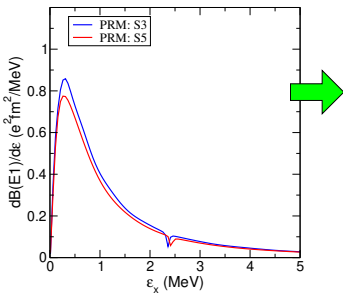
- The extracted $dB(E\lambda)/dE$ distributions are reasonably compatible, but with apparent differences at the peak



CDCC analysis of Coulomb dissociation data

- ⇒ Nuclear excitation not negligible, even for small θ
- ⇒ Nuclear contribution interferes with Coulomb
- ⇒ Higher-order couplings can affect the cross sections
- ⇒ These ingredients can be naturally incorporated within the CDCC method (at the expense of more complexity!)

E.g.: CDCC analysis based on two-body $^{10}\text{Be} + \text{n}$ model:



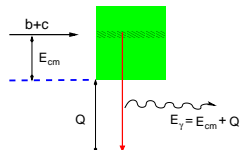
PLB 811 (2020) 135959

- ⇒ Different structure models yield different $B(E1)$ strengths and hence different breakup cross sections
- ⇒ Comparison with the angular distribution evidences the deficiencies of the semiclassical EPM model

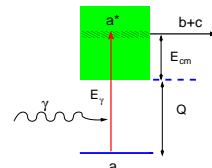


Application to radiative capture reactions

Radiative capture: $b + c \rightarrow a + \gamma$



Photodissociation: $a + \gamma \rightarrow b + c$



⇒ Related by detailed balance:

$$\sigma_{E\lambda}^{(rc)} = \frac{2(2J_a + 1)}{(2J_b + 1)(2J_c + 1)} \frac{k_\gamma^2}{k^2} \sigma_{E\lambda}^{(phot)} \quad (\hbar k_\gamma = E_\gamma/c)$$

⇒ Astrophysical S-factor:

$$S(E_{c.m.}) = E_{c.m.} \sigma_{E\lambda}^{(rc)} \exp[2\pi\eta(E_{c.m.})]$$

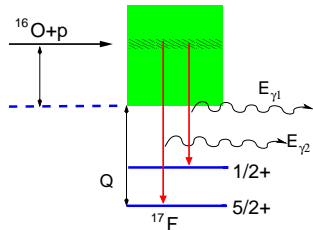
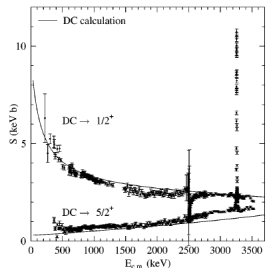
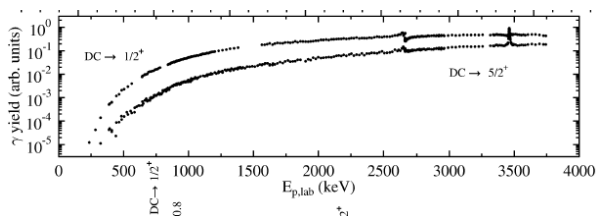
⇒ Capture cross sections are difficult to measure because they are very small at relevant astrophysical energies.



Direct determination of radiative capture cross sections

Example: $p + {}^{16}\text{O} \rightarrow {}^{17}\text{F} + \gamma$

Morlock, PRL79, 3837 (1997)





Indirect determination of radiative capture from Coulomb breakup

⇒ The photodissociation ($\gamma + a \rightarrow b + c$) cross section is related to the $B(E\lambda)$

$$\sigma_{E\lambda}^{\text{photo}} = \frac{(2\pi)^3(\lambda + 1)}{\lambda[(2\lambda + 1)!!]^2} \left(\frac{E_\gamma}{\hbar c} \right)^{2\lambda-1} \frac{dB(E\lambda)}{dE}$$

⇒ Then, in 1st order semiclassical limit, the Coulomb breakup x-section is proportional to photodissociation x-section:

$$\frac{d\sigma(E\lambda)}{d\Omega dE_\gamma} = \frac{1}{E_\gamma} \frac{dn_{E\lambda}}{d\Omega} \sigma_{E\lambda}^{\text{photo}}$$

(Equivalent Photon Method)

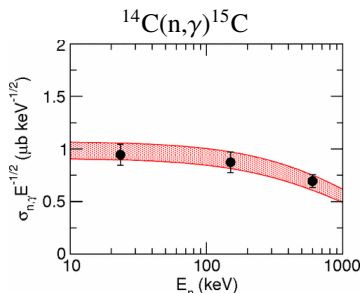
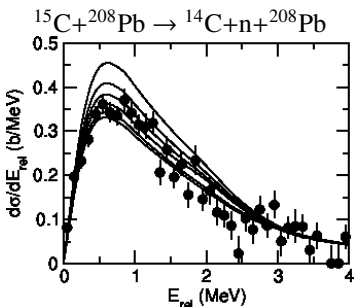
with the virtual photon number

$$\frac{dn_{E\lambda}}{d\Omega} = Z_t^2 \alpha \frac{\lambda[(2\lambda + 1)!!]^2}{(2\pi)^3(\lambda + 1)} \xi^{2(1-\lambda)} \left(\frac{c}{v} \right)^{2\lambda} \frac{df_{E\lambda}}{d\Omega}$$

Radiative capture from Coulomb dissociation experiments

- ☞ Capture reactions have typically small cross sections
 - ☞ As an alternative, one can indirectly obtain the capture cross sections from Coulomb dissociation experiments involving the same two-body projectile:

$$\frac{d\sigma}{d\Omega dE_{c.m.}} \rightarrow \sigma_{E\lambda}^{(\text{phot})} \rightarrow \sigma_{E\lambda}^{(rc)} \rightarrow S(E_{\text{c.m.}})$$

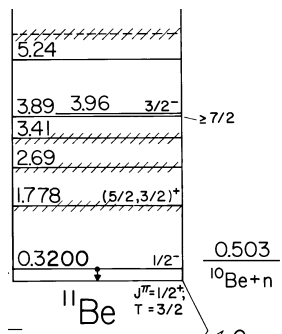


(dots: direct; shaded region: from Coulomb breakup)
 Summers and Nunes, PRC 78, 011601(R), 2008



Exploring structures in the continuum

The continuum spectrum is not “homogeneous”; it contains in general energy regions with special structures, such as resonances and virtual states





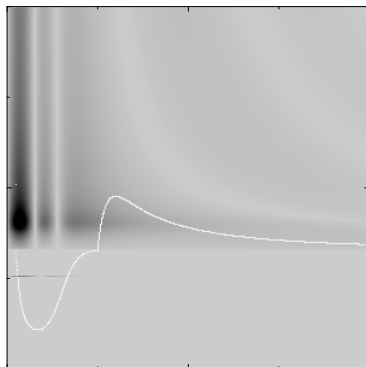
What is a resonance?

- ⇒ It is a **pole** of the S-matrix in the complex energy plane.
- ⇒ It is a structure on the continuum which may, or may not, produce a **maximum in the cross section**, depending on the reaction mechanism and the phase space available.
- ⇒ The resonance occurs in the range of energies for which the **phase shift is close to $\pi/2$** .
- ⇒ In this range of energies, **the continuum wavefunctions is largely localized** within the radial range of the potential.
- ⇒ The continuum wavefunctions are **not square normalizable**. For practical reasons, a normalized wave-packet (or “bin”) can be constructed to represent the resonance.



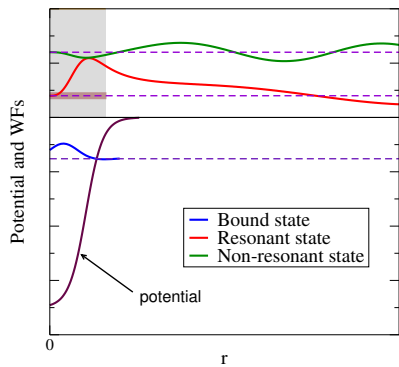
Distinctive features of a resonance

In the energy range of the resonance, the continuum wavefunctions have a large probability of being within the range of the potential.

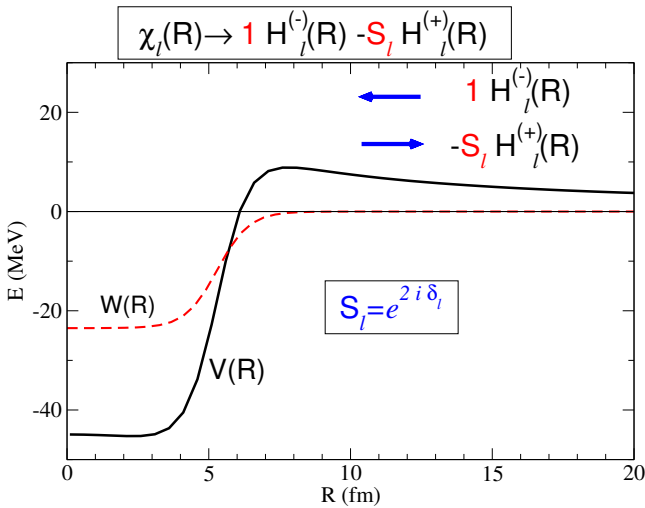


Cuts and areas ordered by size

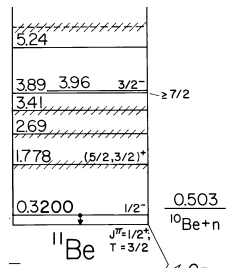
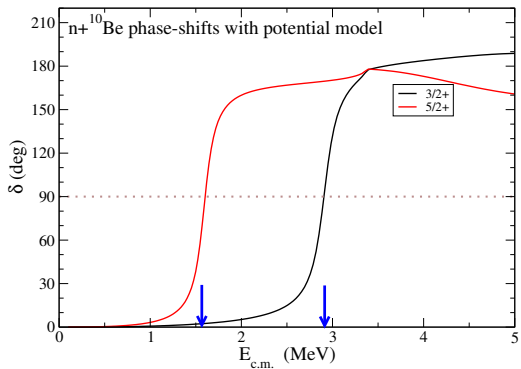
(Courtesy of C. Dasso)



Resonances and phase-shifts

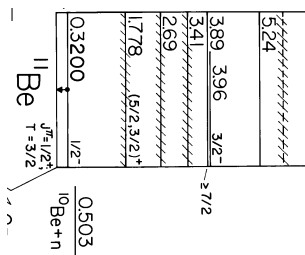
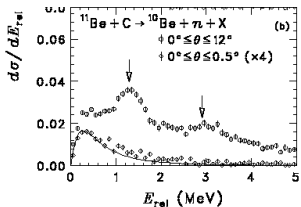


Resonances and phase-shifts

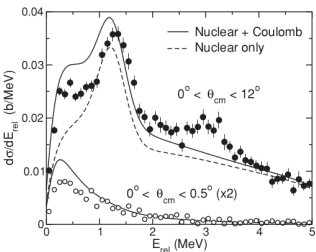
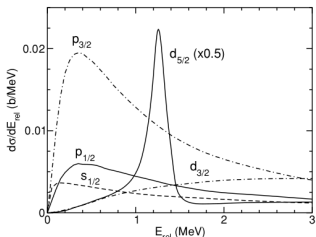


Studying resonances in nuclear breakup experiments

RIKEN data



CDCC analysis



Proposed exercise

Consider a simple two-body model for a one-neutron halo nucleus. For E1 transitions, the electric transition probability is given by

$$\frac{dB(E1)}{dE_c} = \left(\frac{4\pi}{k}\right)^2 \frac{\mu k}{(2\pi)^3 \hbar^2} \frac{3}{4\pi} \left(\frac{Ze}{A}\right)^2 \left| \langle \ell_i 010 | \ell_f 0 \rangle \int dr r^2 \phi_f(k, r) \phi_i(r) \right|^2$$

where μ is the reduced mass of the two-body system, $\phi_i(r)$ is the radial part of the ground-state wavefunction and $\phi_f(k, r)$ is the radial part of the positive-energy state with energy $E_c = \hbar^2 k^2 / 2\mu$ and asymptotic behaviour $\phi_f(k, r) \xrightarrow{r \gg} (kr) j_\ell(kr)$

- >Show that, in the special case in which the final states are approximated by plane waves, the $B(E1)$ distribution is related to the Fourier transform of the ground state wavefunction. Give arguments to justify that, in the case of weakly bound systems, the $B(E1)$ distribution is concentrated at low excitation energies.



Exercises

- In the situation above, the ground state wavefunction can be approximated by its asymptotic form which, for a s -wave configuration, can be written as

$$\phi_i(r) \simeq \sqrt{2k_0} e^{-k_0 r}/r.$$

Give the expression for k_0 in terms of the neutron separation energy (S_n) and the reduced mass of the neutron-core system. Compute it numerically for the ^{11}Be ($^{10}\text{Be}+n$) case.

- Show that, under these approximations, the $B(E1)$ distribution is given by

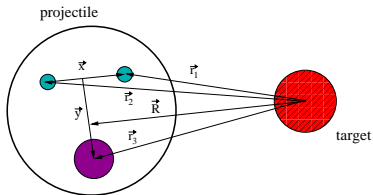
$$\frac{dB(E1)}{dE_c} = \frac{3\hbar^2}{\pi^2\mu} \left(\frac{Ze}{A}\right)^2 \frac{\sqrt{S_n} E_c^{3/2}}{(E_c + S_n)^4}.$$

Hint: $\int_0^\infty dr r^2 j_1(br) e^{-ar} = 2b/(a^2 + b^2)^2$

- Show that the maximum of this $B(E1)$ distribution is located at $E_c = \frac{3}{5}S_n$.

Advanced CDCC applications

Extension to 3-body projectiles



To extend the CDCC formalism, one needs to evaluate the new coupling potentials:

$$V_{n;n'}(\mathbf{R}) = \int d\mathbf{r} \phi_n^*(\mathbf{x}, \mathbf{y}) \{ V_{nt}(\mathbf{r}_1) + V_{nt}(\mathbf{r}_2) + V_{at}(\mathbf{r}_3) \} \phi_{n'}(\mathbf{x}, \mathbf{y})$$

- ☞ $\phi_n(\mathbf{x}, \mathbf{y})$ three-body WFs for bound and continuum states: hyperspherical coordinates, Faddeev, etc (difficult to calculate!)
 - ☞ 4b-CDCC calculations not included in FRESCO; require separate codes to compute the $\phi_n(\mathbf{x}, \mathbf{y})$ wfs (e.g. FACE) and $V_{n,n'}(\mathbf{R})$ potentials

Calculation of three-body states in the HH formalism

$$\Psi^{j\mu}(\rho, \Omega) = \rho^{-5/2} \sum_{\beta} \chi_{\beta}^j(\rho) \mathcal{Y}_{\beta}^{j\mu}(\Omega) \quad \beta \equiv \{K, l_x, l_y, l, S_x, J; I\}$$

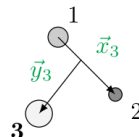
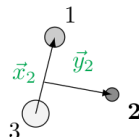
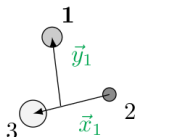
Hyperspherical Harmonics (HH) expansion

hypermomentum \hat{K}

$$\mathcal{Y}_\beta^{j\mu}(\Omega) = \left[\left(\Upsilon_{Klm_l}^{l_x l_y}(\Omega) \otimes \kappa_{S_x} \right)_J \otimes \phi_I \right]_{i\mu}$$

$$\Upsilon_{Klm_1}^{l_x l_y}(\Omega) = \varphi_{\alpha}^{l_x l_y}(\alpha) [Y_{l_x}(\hat{x}) \otimes Y_{l_y}(\hat{y})]_{lm_1}$$

$$\varphi_{\mathcal{L}_x \mathcal{L}_y}^{l_x l_y}(\alpha) = N_K^{l_x l_y} (\sin \alpha)^{l_x} (\cos \alpha)^{l_y} P_n^{l_x + \frac{1}{2}, l_y + \frac{1}{2}}(\cos 2\alpha)$$



Jacobi
coordinates
 $\{x, y, \hat{x}, \hat{y}\}$

Hyperspherical coordinates

$$\{\rho, \alpha, \hat{x}, \hat{y}\}$$

$$\rho = \sqrt{x^2 + y^2}$$

$$\alpha = \arctan \frac{x}{y}$$

oo • ooooo

Calculation of three-body states in the HH formalism

$$\Psi^{j\mu}(\rho, \Omega) = \rho^{-5/2} \sum_{\beta} \chi_{\beta}^j(\rho) \mathcal{Y}_{\beta}^{j\mu}(\Omega) \quad \beta \equiv \{K, l_x, l_y, l, S_x, J; I\}$$

Hyperspherical Harmonics (HH) expansion

hypermomentum \hat{K}

$$\mathcal{Y}_\beta^{j\mu}(\Omega) = \left[\left(\Upsilon_{Klm_l}^{l_x l_y}(\Omega) \otimes \kappa_{S_x} \right)_J \otimes \phi_I \right]_{i\mu}$$

$$\Upsilon_{Klm_l}^{l_x l_y}(\Omega) = \varphi_K^{l_x l_y}(\alpha) [Y_{l_x}(\hat{x}) \otimes Y_{l_y}(\hat{y})]_{lm_l}$$

$$\varphi_{K_x K_y}^{l_x l_y}(\alpha) = N_K^{l_x l_y} (\sin \alpha)^{l_x} (\cos \alpha)^{l_y} P_n^{l_x + \frac{1}{2}, l_y + \frac{1}{2}}(\cos 2\alpha)$$

Hyperradial functions are the solution of the coupled equations:

$$\left[-\frac{\hbar^2}{2m} \left(\frac{d^2}{d\rho^2} - \frac{15/4 + K(K+4)}{\rho^2} \right) - \varepsilon \right] \chi_{\beta}^j(\rho) + \sum_{\beta'} V_{\beta'\beta}^{j\mu}(\rho) \chi_{\beta'}^j(\rho) = 0$$

with coupling potentials $V_{\beta'\beta}^{j\mu}(\rho)$. Model space defined by a given K_{max}



Calculation of three-body states in the HH formalism

$$V_{\beta'\beta}^{j\mu}(\rho) = \left\langle \mathcal{Y}_{\beta}^{j\mu}(\Omega) \middle| V_{12} + V_{13} + V_{23} \middle| \mathcal{Y}_{\beta'}^{j\mu}(\Omega) \right\rangle + \delta_{\beta\beta'} V_{3b}(\rho)$$

- V_{ij} interaction between pairs
central, spin-orbit, spin-spin, tensor. To reproduce binary subsystem
- V_{3b} phenomenological three-body force
diagonal term. Fixed to fine-tune the three-body energies

Pseudo-State (PS) method

$$\chi_{\beta}^j(\rho) = \sum_{i=0}^N C_{i\beta}^j U_{i\beta}(\rho) \quad \text{expanded in } \mathcal{L}^2 \text{ basis}$$

N : number of hyperradial excitations included

$$\mathcal{H}\Psi_n^{j\mu} = \varepsilon_n \Psi_n^{j\mu}$$

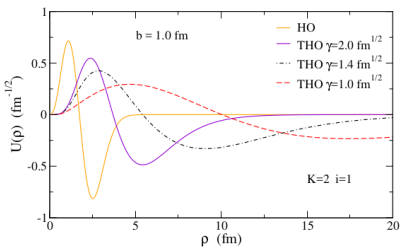
- $\varepsilon_n < 0$ **bound states**
- $\varepsilon_n > 0$ **discretized continuum**

Calculation of three-body states in the HH formalism

Analytical Transformed Harmonic Oscillator (THO) basis

$$U_{i\beta}^{\text{THO}}(\rho) = \sqrt{\frac{ds}{d\rho}} U_{iK}^{\text{HO}}[s(\rho)]$$

$$s(\rho) = \frac{1}{\sqrt{2}b} \left[\frac{1}{\left(\frac{1}{\rho} \right)^4 + \left(\frac{1}{\gamma\sqrt{\rho}} \right)^4} \right]^{\frac{1}{4}}$$

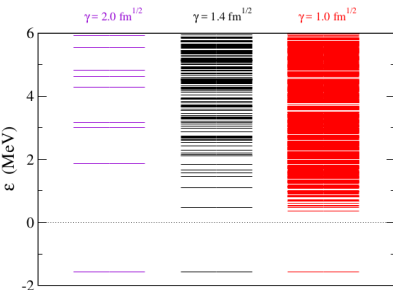


[PRC88(2013)014327]

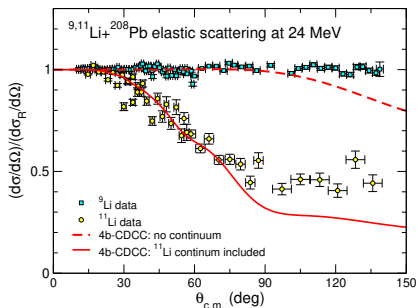
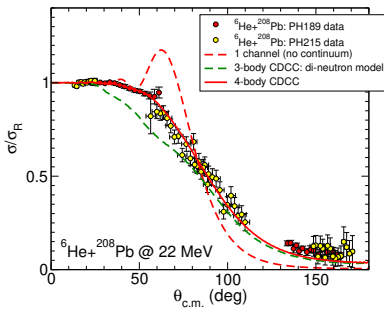
Example:

$\Psi_n^{j\mu}(\rho, \Omega)$ PS spectra, ε_n
 $b = 0.7$ fm

The ratio γ/b controls the density of PS as a function of the energy.



Four-body CDCC calculations for ^6He and ^{11}Li scattering



Data (LLN): NPA803, 30 (2008); PRC 84, 044604 (2011)

Calculations: PRC 80, 051601 (2009)

M Cubero et al, PRL109, 262701 (2012)

N.b.: 1-channel potential considers only g.s. \rightarrow g.s. coupling potential:

$$V_{00}(\mathbf{R}) = \int d\mathbf{r} \phi_{g.s.}^*(\mathbf{x}, \mathbf{y}) \{ V_{nt}(\mathbf{r}_1) + V_{nt}(\mathbf{r}_2) + V_{ct}(\mathbf{r}_3) \} \phi_{g.s.}(\mathbf{x}, \mathbf{y})$$

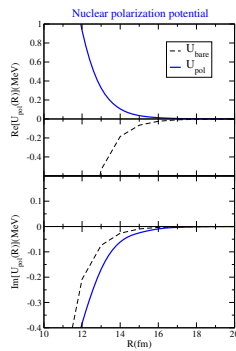
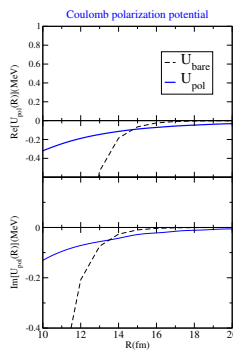


Polarization potential for ${}^6\text{He} + {}^{208}\text{Pb}$: long-range effect

Trivially Equivalent Local Polarization potential (TELP):

$$[E - \varepsilon_0 - \hat{T}_{\mathbf{R}} - V_{0,0}(\mathbf{R})] \chi_0(\mathbf{R}) = \sum_{i \neq 0} V_{i,0}(\mathbf{R}) \chi_i(\mathbf{R}) \equiv U_{\text{TELP}}(\mathbf{R}) \chi_0(\mathbf{R}).$$

Application to ${}^6\text{He} + {}^{208}\text{Pb}$ at 22 MeV

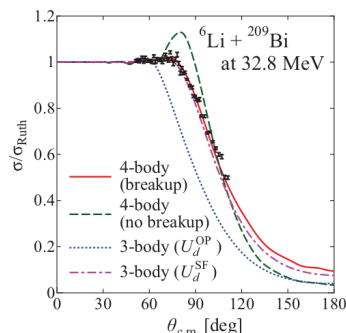
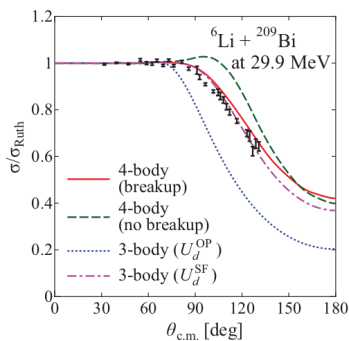


- ⇒ Imaginary part of TELP is long-ranged and absorptive (explains the need for large imaginary diffuseness parameter in OM analysis)
- ⇒ Real part is attractive for the Coulomb potential and repulsive for the nuclear couplings.

Application to ${}^6\text{Li}$ scattering

Example: ${}^6\text{Li} + {}^{209}\text{Bi}$ around Coulomb barrier

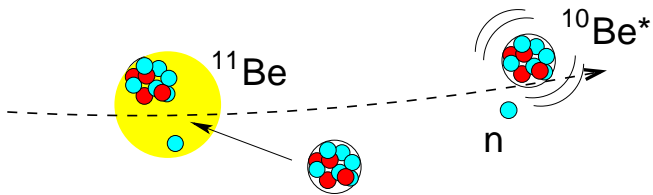
- ⇒ 4-body CDCC: ${}^6\text{Li} = \alpha + p + n$
 - ⇒ 3-body CDCC: ${}^6\text{Li} = \alpha + d$



Watanabe *et al*, PRC 86, 031601(R) (2012)

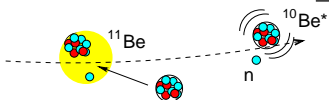
Beyond the strict few-body picture: the effect of core excitation

To what extent can one ignore the dynamics of the core?



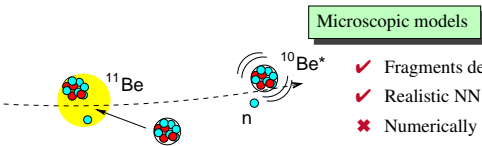
Few-body versus Microscopic

Microscopic models

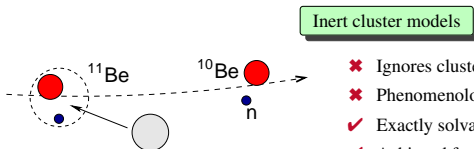


- ✓ Fragments described microscopically
 - ✓ Realistic NN interactions (Pauli properly accounted for)
 - ✗ Numerically demanding / not simple interpretation.

Few-body versus Microscopic

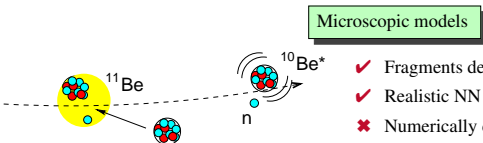


- ✓ Fragments described microscopically
 - ✓ Realistic NN interactions (Pauli properly accounted for)
 - ✗ Numerically demanding / not simple interpretation.

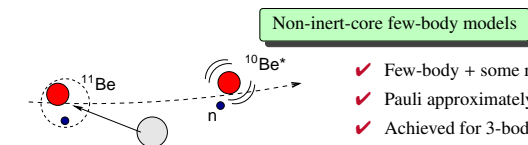


- ✗ Ignores cluster excitations (only few-body d.o.f).
 - ✗ Phenomenological inter-cluster interactions (aprox. Pauli).
 - ✓ Exactly solvable (in some cases).
 - ✓ Achieved for 3-body and 4-body (eg. coupled-channels, Faddeev).

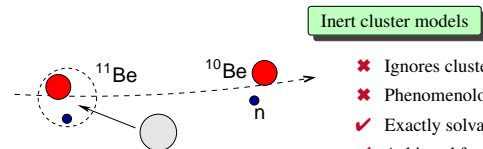
Few-body versus Microscopic



- ✓ Fragments described microscopically
 - ✓ Realistic NN interactions (Pauli properly accounted for)
 - ✗ Numerically demanding / not simple interpretation.



- ✓ Few-body + some relevant collective d.o.f.
 - ✓ Pauli approximately accounted for.
 - ✓ Achieved for 3-body problems (coupled-channels, Faddeev).



- ✖ Ignores cluster excitations (only few-body d.o.f).
 - ✖ Phenomenological inter-cluster interactions (approx. Pauli).
 - ✓ Exactly solvable (in some cases).
 - ✓ Achieved for 3-body and 4-body (eg. coupled-channels, Faddeev).

↑ Many-body
↓ Few-body



Effect of core excitation in scattering observables

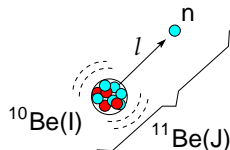
- ⇒ **Elastic** scattering (adiabatic recoil model): K. Horii *et al*, PRC81 (2010) 061602
 - ⇒ Some effects found in ${}^8\text{B} + {}^{12}\text{C}$.
- ⇒ Transfer (DWBA, CCBA, Faddeev): Winfield *et al*, NPA 683 (2001) 48, Fortier *et al*, PLB 461 (1999) 22, Deltuva, Phys.Rev. C 88, 011601 (2013)
- ⇒ Knock-out: Batham et al, PRC71, 064608 (2005)
 - ⇒ Small effect on stripping; large effect on diffraction
- ⇒ Breakup
 - DWBA: Crespo *et al*, PRC83, 044622 (2011), A.M.M. *et al* PRC85, 054613 (2012), A.M.M. and J.A. Lay, PRL109, 232502 (2012)
 - CDCC: Summers *et al*, PRC74, 014606(2006), PRC76,014611 (2007), De Diego *et al*, PRC89, 064609 (2014), PRC 95, 044611 (2017)

How do core excitations affect the breakup of weakly-bound nuclei?

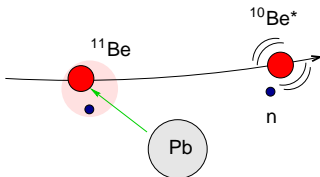
Core excitations will affect:

- ① the **structure** of the projectile \Rightarrow core-excited admixtures

$$\Psi_{JM}(\vec{r}, \xi) = \sum_{\ell,j,I} [\varphi_{\ell,j,I}^J(\vec{r}) \otimes \Phi_I(\xi)]_{JM}$$



- ② the **dynamics** \Rightarrow collective excitations of the ^{10}Be during the collision compete with halo (single-particle) excitations.



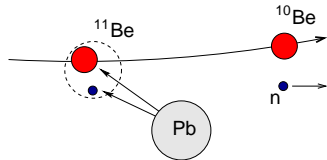
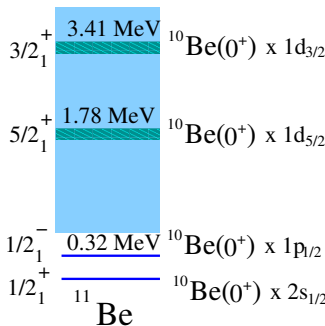
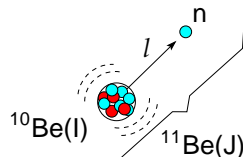
\Rightarrow Both effects have been recently implemented in an extended version of the CDCC formalism (CDCC): Summers *et al*, PRC74 (2006) 014606, R. de Diego *et al*, PRC 89, 064609 (2014)



Core excitation in reactions: *frozen-halo* picture

$$\Psi_{JM}(\vec{r}, \xi) = [\varphi_{\ell,j}^J(\vec{r}) \otimes \Phi_I(\xi)]_{JM}$$

- ⇒ $\varphi_{\ell,j}^J(\vec{r})$ = valence particle wavefunction
- ⇒ $\Phi_I(\xi)$ = core wavefunction (*frozen*)

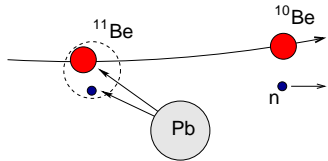
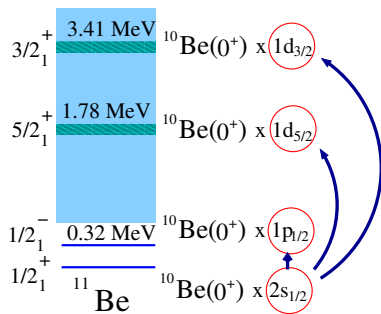
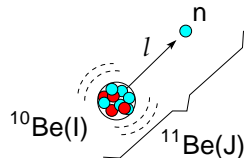




Core excitation in reactions: *frozen-halo* picture

$$\Psi_{JM}(\vec{r}, \xi) = [\varphi_{\ell,j}^J(\vec{r}) \otimes \Phi_I(\xi)]_{JM}$$

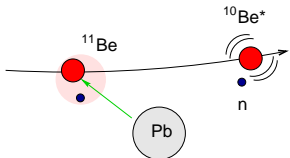
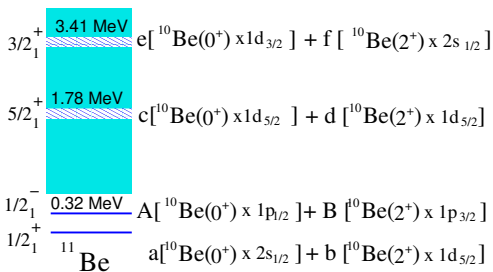
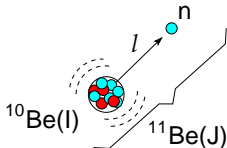
- ⇒ $\varphi_{\ell,j}^J(\vec{r})$ = valence particle wavefunction
- ⇒ $\Phi_I(\xi)$ = core wavefunction (*frozen*)





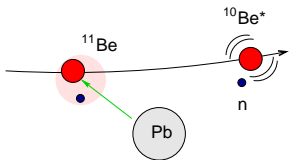
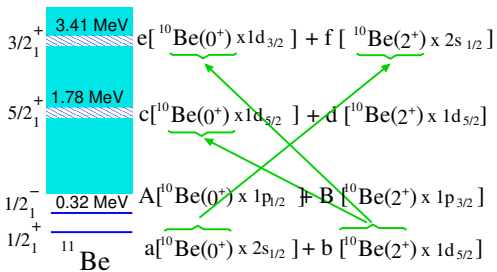
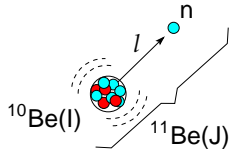
Core excitation mechanism in breakup

$$\Psi_{JM}(\vec{r}, \xi) = \sum_{\ell,j,I} [\varphi_{\ell,j,I}^J(\vec{r}) \otimes \Phi_I(\xi)]_{JM}$$



Core excitation mechanism in breakup

$$\Psi_{JM}(\vec{r}, \xi) = \sum_{\ell, j, I} \left[\varphi_{\ell j, I}^J(\vec{r}) \otimes \Phi_I(\xi) \right]_{JM}$$



☞ Dynamic core excitation contributes to the inelastic/breakup probabilities



Extending CDCC to include core excitations

⇒ Standard CDCC ⇒ use coupling potentials:

$$V_{\alpha;\alpha'}(\mathbf{R}) = \langle \Psi_{J'M'}^{\alpha'}(\vec{r}) | V_{vt}(r_{vt}) + V_{ct}(r_{ct}) | \Psi_{JM}^{\alpha}(\vec{r}) \rangle$$

⇒ Extended CDCC (XCDCC) ⇒ use generalized coupling potentials

$$V_{\alpha;\alpha'}(\mathbf{R}) = \langle \Psi_{J'M'}^{\alpha'}(\vec{r}, \xi) | V_{vt}(r_{vt}) + V_{ct}(r_{ct}, \xi) | \Psi_{JM}^{\alpha}(\vec{r}, \xi) \rangle$$

- ☞ $\Psi_{JM}^{\alpha}(\vec{r}, \xi)$: projectile WFs involving core-excited admixtures (**structure**).
- ☞ $V_{ct}(r_{ct}, \xi)$: non-central potential allowing for core excitations/de-exitations (**dynamic** core excitation).

- Summers *et al*, PRC74 (2006) 014606 (bins)
- R. de Diego *et al*, PRC 89, 064609 (2014) (THO pseudo-states)

Evidences of core excitation in nuclear breakup



Structure part: particle-core model

- ⇒ Particle-plus-core Hamiltonian:

$$H_{\text{proj}} = T_r + h_{\text{core}}(\xi) + V_{vc}(\vec{r}, \xi)$$

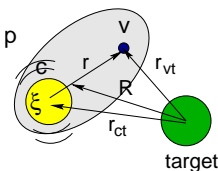
- ⇒ Projectile states expanded in $|\alpha; JM\rangle \equiv |(\ell s)j, I; JM\rangle$ basis:

$$\Psi_{JM}(\vec{r}, \xi) = \sum_{\ell, j, I} R_{\ell, j, I}^J(r) \left[[Y_\ell(\hat{r}) \otimes \chi_s]_j \otimes \Phi_I(\xi) \right]_{JM}$$

- ⇒ The unknowns $R_{\ell, j, I}^J(r)$ can be obtained by direct integration of the Schrödinger equation or by diagonalization in a suitable discrete basis (pseudo-state method).



Valence-core and core-target interactions in a simple collective model



⇒ Valence-core:

$$V_{vc}(\vec{r}, \xi) \simeq V_{vc}^{(0)}(r) - \delta_2 \frac{dV_{vc}^{(0)}}{dr} Y_{20}(\hat{r})$$

⇒ Core-target:

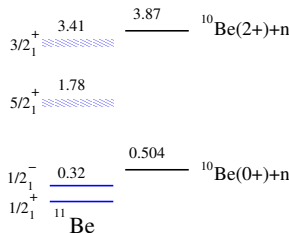
$$V_{ct}(\vec{r}_{ct}, \xi) \simeq \underbrace{V_{ct}^{(0)}(r_{ct})}_{\text{Valence excitation}} - \underbrace{\delta_2 \frac{dV_{ct}^{(0)}}{dr} Y_{20}(\hat{r}_{ct})}_{\text{Core excitation}}$$

$$\delta_2 = \beta_2 R_0 = \text{deformation length}$$

⇒ More sophisticated models for the projectile structure and core-target interaction are possible!



Application to ^{11}Be : spectroscopic factors



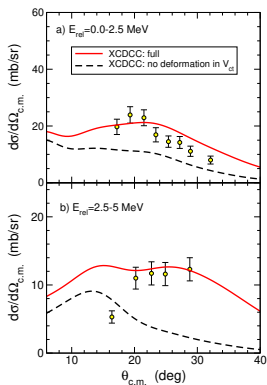
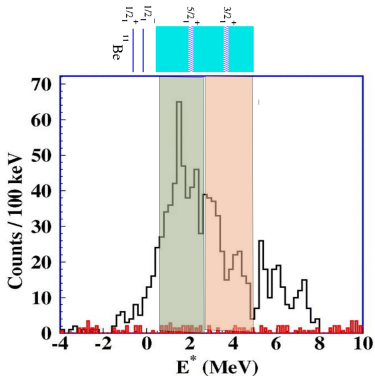
State	Model	$ 0^+ \otimes (\ell s)j\rangle$	$ 2^+ \otimes s_{1/2}\rangle$	$ 2^+ \otimes d_{5/2}\rangle$
$1/2_1^+$ (g.s.)	PRM	0.857	–	0.121
	SM (WBT)	0.76	–	0.184
$5/2_1^+$ (1.78 MeV)	PRM	0.702	0.177	0.112
	SM(WBT)	0.682	0.177	0.095
$3/2_1^+$ (3.41 MeV)	PRM	0.165	0.737	0.081
	SM(WBT)	0.068	0.534	0.167

- ⇒ $1/2_1^+, 5/2_1^+ \Rightarrow$ dominant $^{10}\text{Be}(\text{gs}) \otimes nlj$ configuration
- ⇒ $3/2_1^+ \Rightarrow$ dominant $^{10}\text{Be}(2^+) \otimes 2s_{1/2}$ configuration



Evidence of *dynamical* core excitations in p($^{11}\text{Be},\text{p}'$) at 64 MeV/u (MSU)

Data: Shrivastava et al, PLB596 (2004) 54 (MSU)



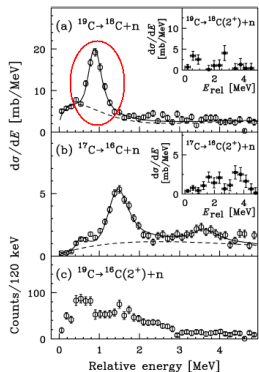
R.de Diego et al, PRC85, 054613 (2014)

- ⇒ $E_{rel}=0\text{--}2.5$ MeV contains $5/2^+$ resonance (expected **single-particle** mechanism)
- ⇒ $E_{rel}=2.5\text{--}5$ MeV contains $3/2^+$ resonance (expected **core excitation** mechanism)

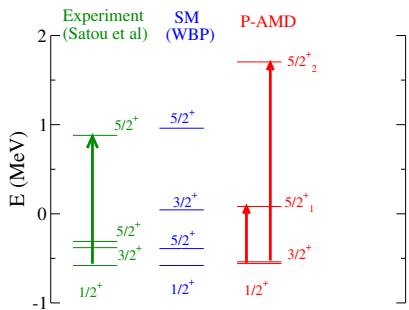
⇒ Dynamical core excitations give additional (and significant!) contributions to breakup

Dominance of *dynamical* core excitations in ^{19}C resonant breakup

$^{19}\text{C} + \text{p} \rightarrow ^{18}\text{C} + \text{n} + \text{p}$ @ 70 MeV/u (RIKEN)



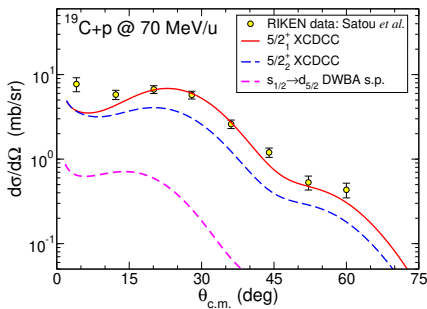
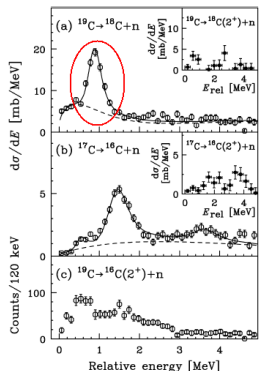
Satou et al, PLB660 (2008) 320



- ⇒ No general consensus about the ^{19}C spectrum.
- ⇒ Resonant peak consistent with $5/2_1^+$, $5/2_2^+$ or even a combination of both.

Dominance of *dynamical* core excitations in ^{19}C resonant breakup

$^{19}\text{C} + \text{p} \rightarrow ^{18}\text{C} + \text{n} + \text{p}$ @ 70 MeV/u (RIKEN)



J.A. Lay et al, PRC 94, 021602 (2016)

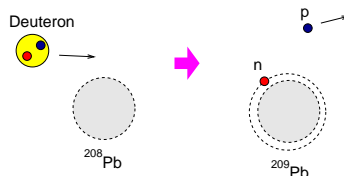
Satou et al, PLB660 (2008) 320

⇒ The core-excitation mechanism gives the dominant contribution to the cross section

Transfer reactions



Outline



Example: $d + ^{208}\text{Pb} \rightarrow p + ^{209}\text{Pb}$

① What do we measure in a transfer reaction?

- ① For a typical transfer reaction (e.g. $d + ^{208}\text{Pb} \rightarrow p + ^{209}\text{Pb}$), one measures the **angular** and **energy** distribution of outgoing fragments (e.g. protons).
- ② Additionally, one may collect information of decay products of ^{209}Pb (e.g. γ -rays, n , p , etc)

② What information can we infer from a transfer reaction?

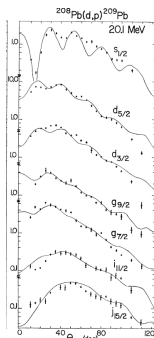
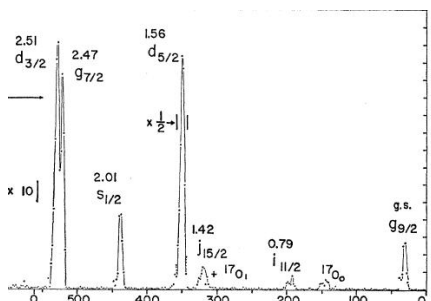
- ① **Excitation energies** of the residual nucleus (^{209}Pb).
- ② **Angular momentum** assignment.
- ③ Single-particle content of populated states (i.e. **spectroscopic factors**).



What do we measure in a transfer reaction?

Example: $d + {}^{208}\text{Pb} \rightarrow p + {}^{209}\text{Pb}$

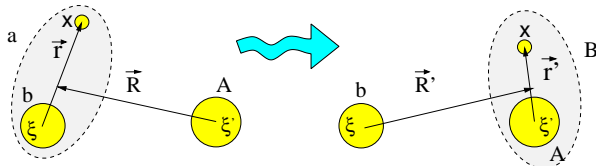
Phys. Rev. 159 (1967) 1039



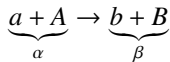
- ☞ The proton energy spectrum shows some peaks which reflect the **energy spectrum** of the residual nucleus (${}^{209}\text{Pb}$).
- ☞ Each peak has a characteristic **angular distribution**, which depends on the structure of the associated state.
- ☞ The population probability will depend on the **reaction dynamics** and on the **structure properties** of these states.

DWBA method for transfer reactions

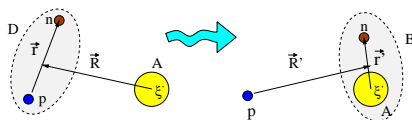
⇒ Transfer process: $\underbrace{(b+x)}_a + A \rightarrow b + \underbrace{(A+x)}_B$



- ⇒ Complications arise with respect to inelastic scattering because now we have two different mass partitions involved



The important (d, p) case



- Introduce auxiliary potentials in entrance ($U_\alpha(\mathbf{R})$) and exit ($U_\beta(\mathbf{R}')$) channels.
- Projectile-target interaction: $V_\beta = V_{pn} + U_{pA} = U_{pB}(\mathbf{R}') + \underbrace{V_{pn} + U_{pA} - U_{pB}}_{\Delta V_\beta} \equiv U_\beta(\mathbf{R}') + \Delta V_\beta$
- Post-form DWBA transition amplitude:

$$\mathcal{T}_{d,p}^{\text{DWBA}} = \int \int \underbrace{\chi_p^{(-)*}(\mathbf{K}_p, \mathbf{R}') \Phi_B(\xi', \mathbf{r}')}_{\text{Final state}} \underbrace{(V_{pn} + U_{pA} - U_{pB})}_{\Delta V_\beta} \underbrace{\chi_d^{(+)}(\mathbf{K}_d, \mathbf{R}) \varphi_d(\mathbf{r}) \phi_A(\xi') d\xi' d\mathbf{r}' d\mathbf{R}'}_{\text{Initial state}}$$

- ⇒ $\chi_{\alpha,\beta}^{(\pm)}$ are distorted waves for entrance and exit channels, obtained with the optical potentials $U_\alpha(\mathbf{R})$, $U_\beta(\mathbf{R}')$
- For medium-mass/heavy targets: $U_{pA} \approx U_{pB} \Rightarrow V_{pn} + U_{pA} - U_{pB} \approx V_{pn}(\mathbf{r})$



(d, p) case: parentage decomposition of target nucleus

⇒ Approximation of the **overlap integral**

$$\int d\xi' \phi_B^*(\xi', \mathbf{r}') \phi_A(\xi') \approx C_{BA}^{\ell j} \varphi_{nA}^{\ell j}(\mathbf{r}')$$

- $C_{BA}^{\ell j}$ = spectroscopic amplitude
- $|C_{BA}^{\ell j}|^2 = S_{BA}^{\ell j}$ = spectroscopic factor
- $\varphi_{nA}^{\ell j}(\mathbf{r}')$ = single-particle wavefunction describing motion of n with respect to A .

$$\mathcal{T}_{d,p}^{\text{DWBA}} = C_{BA}^{\ell j} \int \int \chi_p^{(-)*}(\mathbf{K}_p, \mathbf{R}') \varphi_{nA}^{\ell j,*}(\mathbf{r}') V_{pn}(\mathbf{r}) \chi_d^{(+)}(\mathbf{K}_d, \mathbf{R}) \varphi_d(\mathbf{r}) d\mathbf{r}' d\mathbf{R}'$$

$$\left(\frac{d\sigma}{d\Omega} \right)_{\beta,\alpha} = \frac{\mu_\alpha \mu_\beta}{(2\pi\hbar^2)^2} S_{BA}^{\ell j} \left| \int \int \chi_p^{(-)*}(\mathbf{K}_p, \mathbf{R}') \varphi_{nA}^{\ell j,*}(\mathbf{r}') V_{pn}(\mathbf{r}) \chi_d^{(+)}(\mathbf{K}_d, \mathbf{R}) \varphi_d(\mathbf{r}) d\mathbf{r}' d\mathbf{R}' \right|^2$$

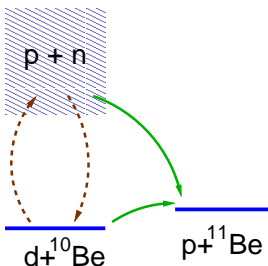
⇒ In DWBA, the (d, p) cross section is proportional to the spectroscopic factor. Comparing the data with DWBA calculations, one can extract the values of $S_{BA}^{\ell j}$

Transfer reactions with weakly bound nuclei



Transfer reactions with weakly bound nuclei

- ⇒ DWBA approximates the total WF by the elastic channel and assumes that the transfer occurs in one step (Born approximation).
- ⇒ For weakly bound projectiles (eg. deuterons), breakup is an important channel and can influence the transfer process.



- ⇒ $\Psi_{\mathbf{K}_d}^{(+)}(\mathbf{R}, \mathbf{r})$ includes breakup components, but these are lost when we make the DWBA approximation ($\Psi^{(+)} \approx \chi_d^{(+)}(\mathbf{K}_d, \mathbf{R})\varphi_d(\mathbf{r})$) \Rightarrow need to go beyond DWBA



Adiabatic distorted wave approximation (ADWA)

- ⇒ $\chi_d^{(+)}(\mathbf{K}_d, \mathbf{R})$ describes deuteron elastic scattering but, for the (d, p) transfer matrix element, we need only $\Psi_{\mathbf{K}_d}^{(+)}(\mathbf{R}, \mathbf{r})$ for small $|\mathbf{r}|$
- ⇒ R.C. Johnson and col. have derived an approximation of $\Psi_{\mathbf{K}_d}^{(+)}(\mathbf{R}, \mathbf{r})$ valid for $r \approx 0$, which includes the effect of deuteron breakup effectively (**adiabatic approx.**):

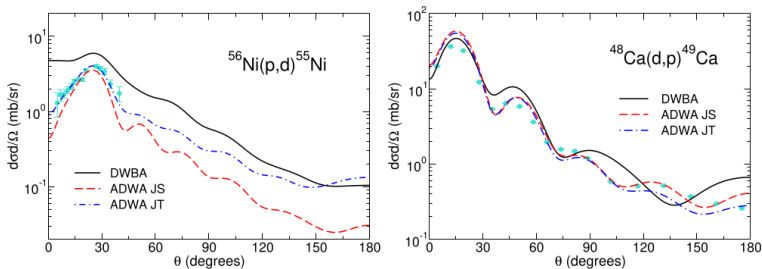
① Zero-range approximation (Johnson-Soper): [(Johnson,Soper,PRC1, 976 (1970)]

$$U^{JS}(R) = U_{pb}(R) + U_{nb}(R) \Rightarrow \chi_d^{JS}(\mathbf{R})$$

② Finite-range version (Johnson-Tandy): [Johnson & Tandy, NPA235 (1974) 56]

$$U^{JT}(R) = \frac{\langle \varphi_{pn}(\mathbf{r}) | V_{pn} (U_{nb} + U_{pb}) | \varphi_{pn}(\mathbf{r}) \rangle}{\langle \phi_{pn}(\mathbf{r}) | V_{pn} | \phi_{pn}(\mathbf{r}) \rangle}$$

DWBA vs ADWA



From Timofeyuk and, Progress in Particle and Nuclear Physics 111 (2020) 103738

CDCC-BA approximation

- ⇒ Exact transition amplitude for a general $A(d, p)B$ process:

$$\mathcal{T}_{d,p}^{\text{CDCC}} = C_{BA}^{\ell j} \int \int \chi_p^{(-)*}(\mathbf{K}_p, \mathbf{R}') \varphi_{nA}^{\ell j,*}(\mathbf{r}') V_{pn}(\mathbf{r}) \underbrace{\Psi_{\mathbf{K}_a}^{(+)}(\mathbf{R}_\alpha, \xi_\alpha)}_{d\mathbf{r}' d\mathbf{R}'}$$

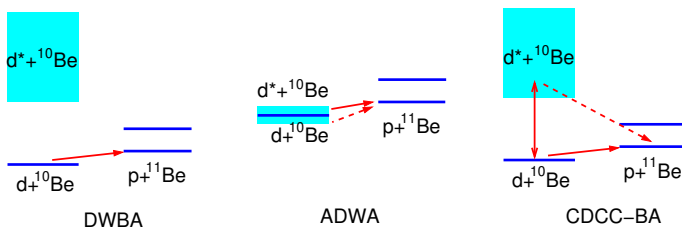
- ⇒ Use CDCC approximation for $\Psi_{\mathbf{k}}^{(+)}$:

$$\Psi_{\mathbf{K}_a}^{(+)} \approx \Psi^{\text{CDCC}} = \underbrace{\chi_0(\mathbf{R})\phi_0(\mathbf{r})}_{\text{elastic}} + \underbrace{\sum_{n',j,\pi} \phi_{n'}^{j\pi}(k_{n'}, \mathbf{r}) \chi_{n'j,\pi}(\mathbf{R})}_{\text{breakup}}$$

- Unlike the DWBA and ADWA methods, coupling to deuteron breakup states is included explicitly.



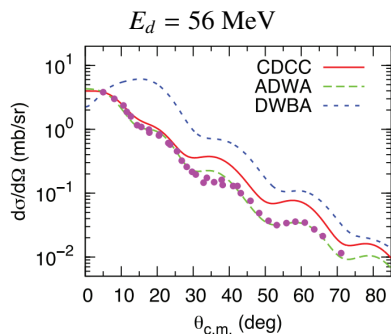
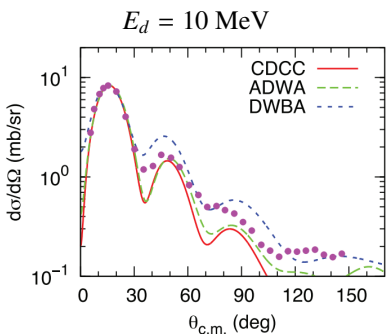
DWBA, ADWA and CDCC-BA compared



Gómez-Camacho and A.M.M., *A Pedestrian Approach to the Theory of Transfer Reactions: Application to Weakly-Bound and Unbound Exotic Nuclei*, Lecture Notes in Physics, vol 879.

DWBA vs APWA vs CDCC

Example: $^{58}\text{Ni}(\text{d},\text{p})^{59}\text{Ni}$



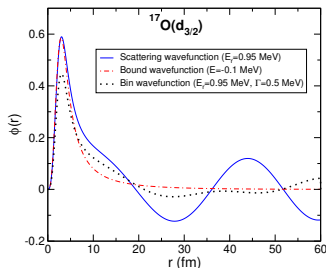
CDCC and ADWBA provide better description of the data and lead also to more realistic spectroscopic information (e.g. spectroscopic factors)

Pang *et al*, PRC 90, 044611 (2014)

Exploring resonances from transfer reactions

- Calculation of transfer to unbound states in DWBA and ADWA poses numerical problems due to the oscillatory behaviour of unbound wavefunctions.
 - A regularization method must be applied:
 - Representing the resonance by a weakly bound state with the same quantum numbers
 - Vincent & Fortune contour integration in the complex radius plane ([PRC2 \(1970\) 782](#))
 - Representing the resonance by a continuum *bin*

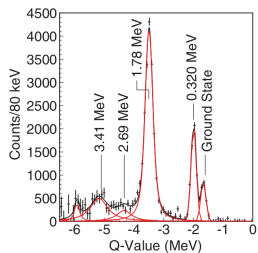
E.g.: $d_{3/2}$ resonance in ^{17}O resonance at $E_r = 0.95 \text{ MeV}$





Application of ADWA populating unbound states

E.g.: ^{11}Be resonance at $E_x = 1.78 \text{ MeV}$ from $^{10}\text{Be}(\text{d},\text{p})^{11}\text{Be}$



Schmitt et al, PRC88, 064612 (2013)

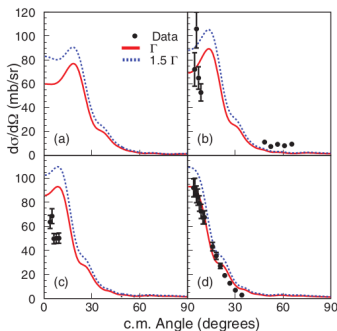
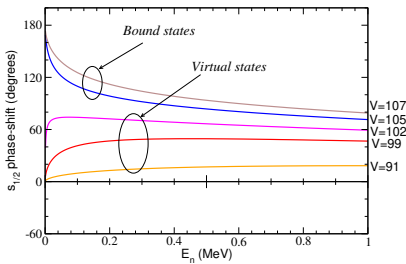


FIG. 8. (Color online) Differential cross sections are presented for transfer to the first resonance in ^{11}Be at 1.78 MeV via the $^{10}\text{Be}(\text{d},\text{p})$ reaction in inverse kinematics at deuteron energies of (a) 12 MeV , (b) 15 MeV , (c) 18 MeV , and (d) 21.4 MeV . The curves are from FR-ADWA calculations using (solid line) an energy bin that is the same width as for the resonance used in the calculation and (dotted line) with a width 1.5 times that value. At 12 MeV the protons were too low in energy to extract an angular distribution.

Virtual states

- ⇒ Neutrons in s -wave cannot produce resonant states (no barrier)
 - ⇒ Still, they can exhibit distinctive structures, characterized by a rapid increase of the phase-shift near zero energy (**virtual states**). This behaviour is commonly characterized in terms of the **scattering length**:

$$a_s = - \lim_{k \rightarrow 0} \tan \frac{\delta(k)}{k}$$



Levinson theorem:

$$\delta_\ell(E_n = 0) \rightarrow n\pi$$

(n =number of bound states for partial wave ℓ)



Resonances and virtual states in the complex energy/momentum plane

- ⇒ A **bound state** is a normalizable solution of the Schrödinger equation for a imaginary momentum $+i|k|$ and (negative) energy: $E_s = \hbar^2(+i|k|)^2/2\mu = -\hbar^2|k|^2/2\mu$.
- ⇒ A **virtual state** is a non-normalizable solution of the Schrödinger equation for a imaginary momentum $-i|k|$ and (negative) energy: $E_s = \hbar^2(-i|k|)^2/2\mu = -\hbar^2|k|^2/2\mu$.

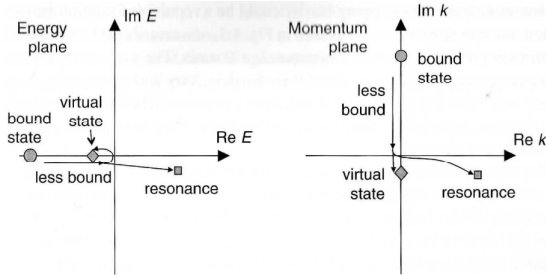
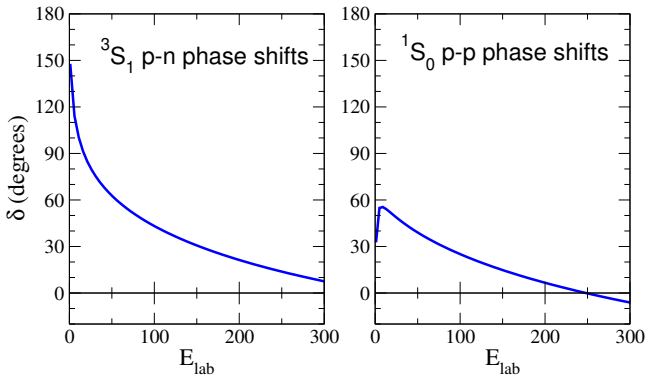


Fig. 3.4. The correspondences between the energy (left) and momentum (right) complex planes. The arrows show the trajectory of a bound state caused by a progressively weaker potential: it becomes a resonance for $L > 0$ or when there is a Coulomb barrier, otherwise it becomes a virtual state. Because $E \propto k^2$, bound states on the positive imaginary k axis and virtual states on the negative imaginary axis both map onto the negative energy axis.

(figure borrowed from Thompson & Nunes' book)

Bound vs virtual (anti-bound) states in the N-N system

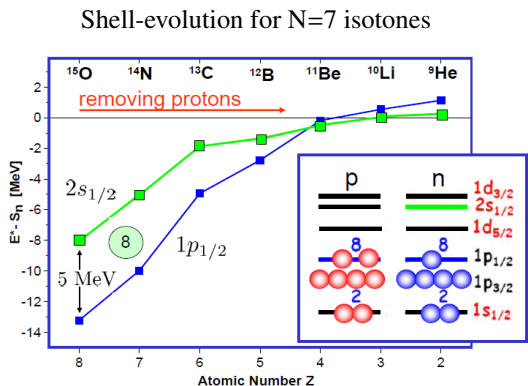
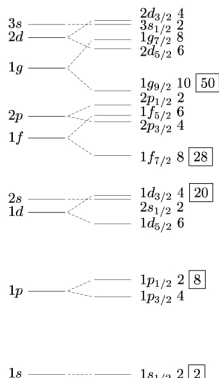


- ⇒ $p - n$: $\delta(E) \xrightarrow{E \rightarrow 0} \pi \Rightarrow$ one-bound state (deuteron)
 - ⇒ $p - p, n - n$: no bound states, but they do have an anti-bound (virtual) state.
 - ⇒ $p - p$: δ becomes negative for large $E \Rightarrow$ evidence of repulsive core!



Spectroscopy in the continuum: shell evolution with neutron/proton asymmetry

⇒ Systematic studies of shell evolution requires extensions to the continuum



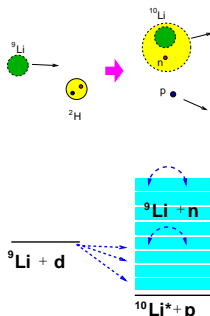
1s —————— 1s_{1/2} 2 [2]

From: P.G. Hansen and J.A. Tostevin, Ann Rev Nucl Part Sci 53 (2003) 219

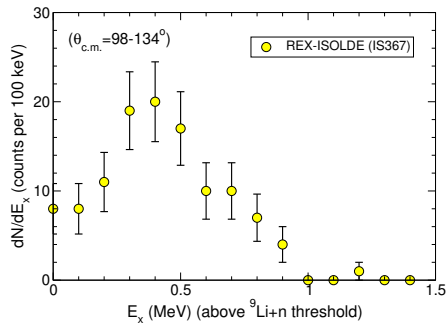
SM explanation: Otsuka et al, PRL95,232502(2005)

Spectroscopy in the continuum: the ${}^{10}\text{Li}$ case

- Detected protons carry information on the ${}^9\text{Li} + n$ excitation spectrum.



H.P. Jeppesen et al, PLB642 (2006) 449

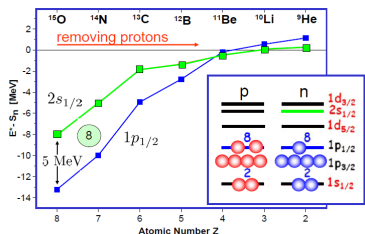


Populating resonances via transfer reactions ${}^9\text{Li}(\text{d},\text{p}){}^{10}\text{Li}^*$

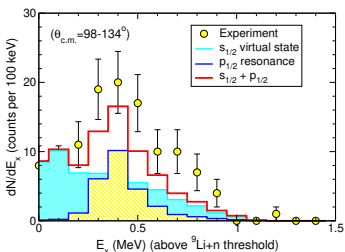
⇒ Prior form transition amplitude:

$$\mathcal{T}_{if} = \langle \Psi_f^{(-)} | V_{nA} + U_{pA} - U_{dA} | \phi_d(\vec{r}) \chi_{dA}^{(+)}(\vec{R}) \rangle$$

⇒ $\Psi_f^{(-)}$, describing $\text{p}+{}^{10}\text{Li}$, approximated by a CDCC expansion in terms of $n+{}^9\text{Li}$ states



From: P.G. Hansen and J.A. Tostevin, Ann Rev Nucl Part Sci 53 (2003) 219



⇒ $p_{1/2}$ resonance (1^+ or 2^+): $E_r \simeq 0.38$ MeV, $\Gamma = 0.2$ MeV

⇒ $s_{1/2}$ virtual state (1^- or 2^-): $a_s \simeq -24$ fm

Coupled-Reaction Channels (CRC) method

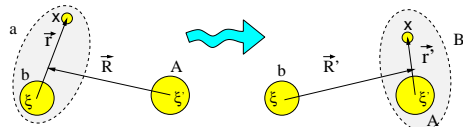


Motivation of the CRC method

- ⇒ The DWBA method includes transfer couplings to first order in the residual interaction (ΔV).
- ⇒ Transfer couplings should affect the elastic channel, but this effect is not considered in DWBA
- ⇒ When couplings are strong, higher orders may be important.

Post and prior Hamiltonians

Transfer process: $\underbrace{(b+x)}_a + A \rightarrow b + \underbrace{(b+x)}_B$



⇒ Full Hamiltonian:

- Prior form: $\xi_\alpha = \{\xi, \xi', \mathbf{r}\}$

$$H = \hat{T}_{\mathbf{R}} + H_a(\xi_\alpha) + V_\alpha(\mathbf{R}, \mathbf{r}) = \hat{T}_{\mathbf{R}} + \underbrace{H_a(\xi, \mathbf{r})}_{H_a(\xi_\alpha)} + \underbrace{H_A(\xi') + V_{xA} + U_{bA}}_{V_\alpha(\mathbf{R}, \mathbf{r})}$$

- Post form: $\xi_\beta = \{\xi, \xi', \mathbf{r}'\}$

$$H = \hat{T}_{\mathbf{R}'} + H_\beta(\xi_\beta) + V_\beta(\mathbf{R}', \mathbf{r}') = \hat{T}_{\mathbf{R}'} + \underbrace{H_b(\xi) + H_B(\xi', \mathbf{r}')}_{H_\beta(\xi_\beta)} + \underbrace{V_{xb} + U_{bA}}_{V_\beta(\mathbf{R}', \mathbf{r}')}$$

Coupled Reaction Channels: two-channels case

⇒ Trial model wavefunction:

$$\Psi = \underbrace{\phi_a(\xi, \mathbf{r})\phi_A(\xi')\chi_\alpha(\mathbf{R}_\alpha)}_{\Phi_\alpha(\xi_\alpha)} + \underbrace{\phi_b(\xi)\phi_B(\xi', \mathbf{r}')\chi_\beta(\mathbf{R}_\beta)}_{\Phi_\beta(\xi_\beta)}$$

⇒ Coupled-reaction channels (CRC) equations: $[H - E]\Psi = 0$

$$\begin{aligned} [E - \varepsilon_\alpha - T_R - U_\alpha(\mathbf{R}_\alpha)]\chi_\alpha(\mathbf{R}_\alpha) &= \int d\mathbf{R}_\beta K_{\alpha\beta}(\mathbf{R}_\alpha, \mathbf{R}_\beta)\chi_\beta(\mathbf{R}_\beta) \\ [E - \varepsilon_\beta - T_R - U_\beta(\mathbf{R}_\beta)]\chi_\beta(\mathbf{R}_\beta) &= \int d\mathbf{R}_\alpha K_{\alpha\beta}(\mathbf{R}_\alpha, \mathbf{R}_\beta)\chi_\alpha(\mathbf{R}_\alpha) \end{aligned}$$

⇒ Non-local kernels:

$$\begin{aligned} K_{\alpha\beta}(\mathbf{R}_\beta, \mathbf{R}_\alpha) &= \int d\xi d\xi' d\mathbf{r} \phi_a^*(\xi, \mathbf{r})\phi_A^*(\xi')(H - E)\phi_b(\xi)\phi_B(\xi', \mathbf{r}') \\ &\equiv \int d\xi_\alpha \Phi_\beta^*(\xi_\beta)(H - E)\Phi_\alpha(\xi_\alpha) \end{aligned}$$

⇒ CRC equations have to be solved iteratively due to NL kernels.

Evaluation of the non-local kernels

- ⇒ In the NL kernels, H can be replaced by either H^{prior} or H^{post}
- ⇒ E.g., for $H = H^{\text{prior}}$:

$$K_{\alpha\beta} = I_{\alpha\beta}^{\text{prior}} + N_{\alpha\beta}^{\text{prior}}$$

- Interaction kernel:

$$I_{\alpha\beta}^{\text{prior}} = J_{\alpha\beta} \int d\xi_\alpha \Phi_\beta^*(\xi_\beta) (V_\alpha - U_\alpha) \Phi_\alpha(\xi_\alpha)$$

- Non-orthogonality kernel:

$$N_{\alpha\beta}^{\text{prior}} = J_{\alpha\beta} [T_{\mathbf{R}} + U_\alpha - (E - \varepsilon_\alpha)] \int d\xi_\alpha \Phi_\beta^*(\xi_\beta) \Phi_\alpha(\xi_\alpha)$$

Coupled radial equations

- ⇒ As in other CC applications, the total WF is expanded in partial waves, leading to a set of coupled radial differential equations:

$$\begin{aligned} \left[E_{\kappa p t} - T_{\kappa L}(R_\kappa) - U_\kappa(R_\kappa) \right] f_\alpha(R_\kappa) &= \sum_{\alpha', \Gamma > 0} i^{L' - L} V_{\alpha:\alpha'}^\Gamma(R_{\kappa'}) f_{\alpha'}(R_{\kappa'}) \\ &+ \sum_{\alpha', \kappa' \neq \kappa} i^{L' - L} \int_0^{R_m} V_{\alpha:\alpha'}(R_\kappa, R_{\kappa'}) f_{\alpha'}(R_{\kappa'}) dR_{\kappa'} \end{aligned}$$

- Asymptotic kinetic energies: $E_{\kappa p t} = E + Q_\kappa - \epsilon_p - \epsilon_t$
- $R_\kappa, R_{\kappa'} =$ projectile-target radial coordinates in partitions k, k' .
- $V_{\alpha:\alpha'}^\Gamma(R_{\kappa'}) =$ coupling potential of multipolarity Γ within partition k' (local)
- $V_{\alpha:\alpha'}(R_\kappa, R_{\kappa'}) =$ transfer coupling potentials (nonlocal)

- ⇒ Boundary conditions:

$$f_\alpha(R_{\kappa'}) \rightarrow \frac{i}{2} \left[\delta_{\alpha\alpha_0} H_{L\eta_\alpha}^{(-)}(K_\alpha R_\kappa) - S_{\alpha_0\alpha} H_{L\eta_\alpha}^{(+)}(K_\alpha R_\kappa) \right]$$

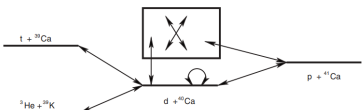
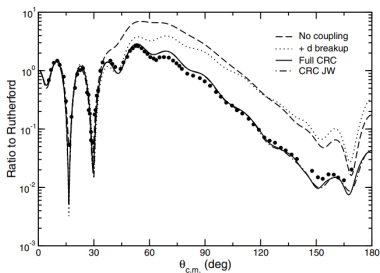
Some remarks on CRC calcultions



- ⇒ For each transfer coupling, we need to provide the appropriate spectroscopic amplitude. Results will depend on its phase!
- ⇒ The diagonal potential describing each channel will not coincide with the optical potential describing elastic scattering in that channel, since the effect of some channels are already taken into account explicitly.

Comparison with data

Example: $d + {}^{40}\text{Ca}$ $E_d = 58 \text{ MeV}$



- ⇒ Full CRC calculation includes coupling to deuteron breakup, (d, t) transfer and $(d, 3He)$ transfer
 - ⇒ The final potential employed for the $d + ^{40}\text{Ca}$ differs from that used in the one-channel optical model case.

Keeley & Mackintosh, PRC77, 054603 (2008)

DWBA approximation from CRC

⇒ Iterative solution of the CRC equations:

$$\begin{aligned}[E - \varepsilon_\alpha - T_R - U_\alpha(\mathbf{R}_\alpha)]\chi_\alpha(\mathbf{R}_\alpha) &\approx 0 \\ [E - \varepsilon_\beta - T_R - U_\beta(\mathbf{R}_\beta)]\chi_\beta(\mathbf{R}_\beta) &\approx \int d\mathbf{R}_\alpha K_{\alpha,\beta}(\mathbf{R}_\alpha, \mathbf{R}_\beta)\chi_\alpha(\mathbf{R}_\alpha)\end{aligned}$$

⇒ DWBA scattering amplitude (prior):

$$f_{\beta,\alpha}^{\text{DWBA}} = -\frac{\mu_\beta}{2\pi\hbar^2} \int \int \widetilde{\chi}_\beta^{(-)*}(\mathbf{R}_\beta)(\phi_b\phi_B|V_{\text{prior}}|\phi_a\phi_A)\widetilde{\chi}_\alpha^{(+)}(\mathbf{R}_\alpha)d\mathbf{R}_\alpha d\mathbf{r}$$

⇒ Distorted waves:

$$\begin{aligned}[E - \varepsilon_\alpha - T_R - U_\alpha(\mathbf{R}_\alpha)]\widetilde{\chi}_\alpha(\mathbf{R}_\alpha) &= 0 \\ [E - \varepsilon_\beta - T_R - U_\beta(\mathbf{R}_\beta)]\widetilde{\chi}_\beta(\mathbf{R}_\beta) &= 0\end{aligned}$$

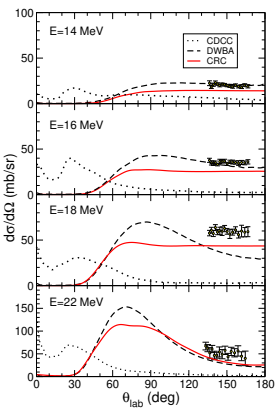
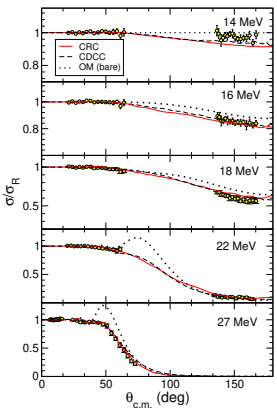
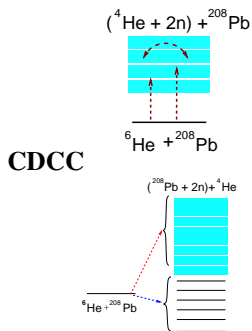
⇒ Structure form-factor:

$$(\phi_b\phi_B|V_{\text{prior}}|\phi_a\phi_A) \equiv \int d\xi d\xi' \phi_b(\xi)\phi_B(\xi', \mathbf{r}')V_{\text{prior}}\phi_a(\xi, \mathbf{r})\phi_A(\xi')$$



Application of CRC method to weakly-bound nuclei

Example: $^6\text{He} + ^{208}\text{Pb}$



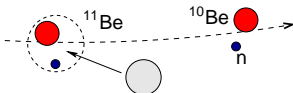
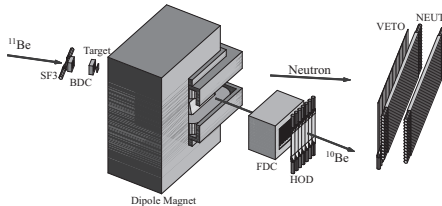
- ⇒ CDCC includes coupling to ^6He continuum states. It describes elastic scattering but not inclusive α 's.
- ⇒ CRC includes coupling to $^{208}\text{Pb} + 2n$ states. Reproduces both elastic scattering and α production.
- ⇒ CRC accounts for transfer and nonelastic breakup processes, not included in CDCC.



The problem of inclusive breakup

Motivation

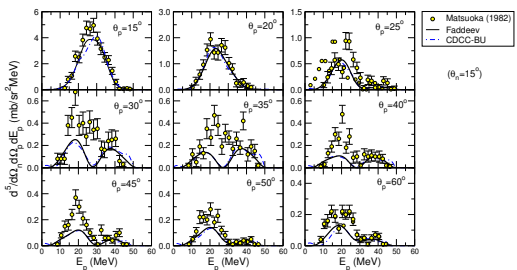
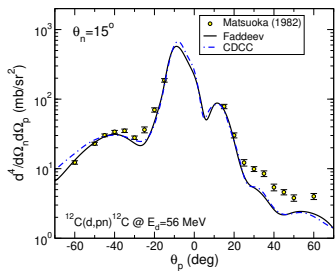
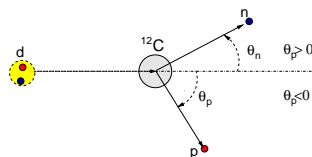
- Weakly-bound nuclei are known to break up easily in collisions with other nuclei due to the nuclear and Coulomb fields.
- When all fragments following dissociation are observed (**exclusive breakup**) different models have been developed and successfully applied: DWBA, CDCC, Faddeev, etc
- Full-kinematical measurements require dedicated experimental setups which are particularly involved when neutron detection is required:



Fukuda et al, PRC 70, 054606 (2004)

Deuteron exclusive breakup

Example: $d + {}^{12}\text{C} \rightarrow p + n + {}^{12}\text{C}$ @ 56 MeV Matsuoka et al, NPA391, 357 (1982)

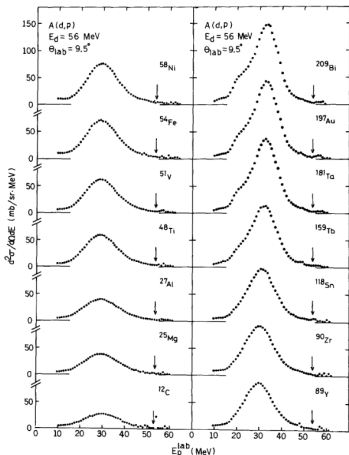


Calc.: Deltuva et al, PRC76, 064602 (2007)



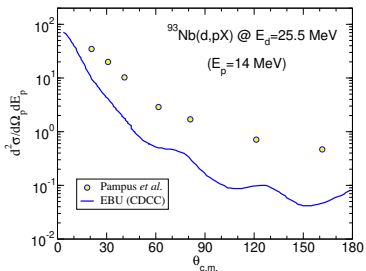
Inclusive deuteron breakup

$d + A \rightarrow p + X @ 56 \text{ MeV}$



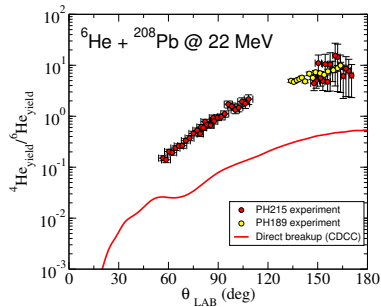
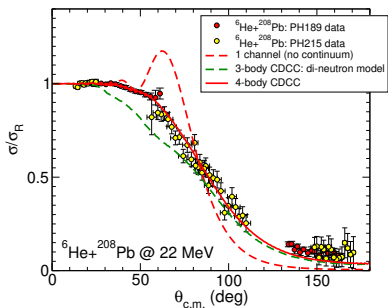
Data: Matsuoka et al, NPA345 (1980) 1

$d + {}^{93}\text{Nb} \rightarrow p + X$



Data: Pampus et al, NPA311, 141 (1978)

Inclusive α production in ${}^6\text{He}$ scattering

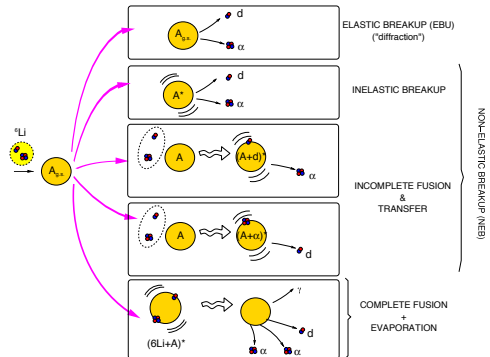


Data (LLN): Sánchez-Benítez et al, NPA 803, 30 (2008) L. Acosta et al, PRC 84, 044604 (2011), D. Escrig et al., NPA 792 (2007) 2

Calculations: Rodríguez-Gallardo et al, PRC 80, 051601 (2009)

CDCC reproduces elastic scattering, but not inclusive α 's.

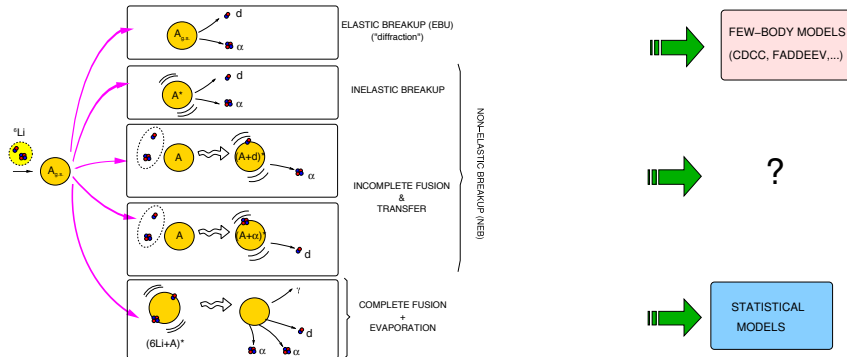
Elastic and nonelastic “breakup” modes: the A(${}^6\text{Li},\alpha$)X example



⇒ For a reaction of the form $a (= b + x) + A \rightarrow b + \text{anything}$

$$\sigma_b = \sigma_{EBU} + \sigma_{NEB} + \sigma_{CN}$$

Elastic and nonelastic “breakup” modes: the A(${}^6\text{Li},\alpha$)X example



⇒ For a reaction of the form $a (= b + x) + A \rightarrow b + \text{anything}$

$$\sigma_b = \sigma_{EBU} + \sigma_{NEB} + \sigma_{CN}$$



Explicit evaluation of inclusive cross sections

- ⇒ Inclusive breakup could in principle be evaluated computing all contributing processes using standard reaction methods, such as DWBA or CRC.
- ⇒ ...however, this procedure has serious shortcomings:
 - Final $x+A$ states span a wide range of excitation energies and spins, so the number of populated states will in general be huge.
 - A significant part of the inclusive spectrum corresponds to $x-A$ continuum.
 - An explicit calculation would require a detailed knowledge of the populated states: spin/parity, spectroscopic factors, . . . , which are poorly known above a few MeV of excitation energy
 - Final states will include, in addition to direct processes, partial fusion (“incomplete fusion”), which are not easily accounted for by standard direct reaction theories.

Inclusive breakup models based on closed-form formulas provide an efficient (and elegant) alternative which exploit the fact that nonelastic $x - A$ processes are encoded in the imaginary part of the U_{xA} optical potential.

Searching in the eighties for inclusive breakup models

- Baur & co: DWBA sum rule with surface approximation.
 - Baur et al, PRC21, 2668 (1980).
 - Hussein & McVoy: extraction of singles cross section combining the spectator model with sum-rule over final states.
 - Nucl. Phys. A445, 124 (1985).
 - Ichimura, Austern, Vincent (IAV): Post-form DWBA.
 - Ichimura, Austern, Vincent, PRC32, 431 (1985).
 - Austern *et al*, Phys. Rep. 154, 125 (1987).
 - Udagawa, Tamura (UT): prior-form DWBA.
 - Udagawa and Tamura, PRC24, 1348 (1981).
 - Udagawa, Lee, Tamura, PLB135, 333 (1984).



Two-body case: optical model potential

- ⇒ **Problem:** describe $a + A$ scattering in a restricted (projected) modelspace (the P space) consisting of the projectile and target ground states without explicit inclusion of other states:

$$\Psi = \underbrace{\Psi_P}_{\text{elastic}} + \underbrace{\Psi_Q}_{\text{non-elastic}}$$

- ⇒ Schrodinger equation in modelspace:

$$[T + \mathcal{V}] \Psi_P = E \Psi_P$$

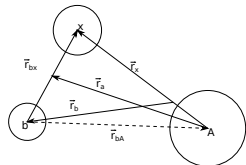
$$\mathcal{V} = \underbrace{V_{PP}}_{\text{Bare interaction}} + V_{PQ} \underbrace{\frac{1}{E - H_{QQ} + i\epsilon}}_{\text{"Polarization" potential}} V_{QP}$$

- ⇒ \mathcal{V} too complicated ⇒ usually replaced by some energy-averaged optical potential U_a (complex)
- ⇒ Asymptotically, Ψ_P contains only the elastic channel so it provides only $a + A$ elastic scattering
- ⇒ However, in virtue of the optical theorem, it provides also the total reaction cross section:

$$\sigma_{\text{reac}} = -\frac{2}{\hbar v_a} \langle \Psi_P | \text{Im}[U_a] | \Psi_P \rangle$$

Inclusive breakup models

- ⇒ Inclusive reaction $\underbrace{(b + x)}_a + A \rightarrow b + (x + A)^*$
- ⇒ b singles cross section: $\sigma_b^{inc} = \sigma_b^{\text{EBU}} + \sigma_b^{\text{NEB}}$



- ⇒ EBU: $a + A \rightarrow b + x + A_{\text{g.s.}}$ can be computed with CDCC, DWBA, etc
- ⇒ σ_b^{NEB} can be interpreted as the absorption occurring in the $x + A$ channel:

$$\frac{d\sigma^{\text{NEB}}}{d\Omega_b dE_b} = -\frac{2}{\hbar v_a} \rho_b(E_b) \langle \varphi_x(\vec{k}_b) | W_{xA} | \varphi_x(\vec{k}_b) \rangle \quad W_{xA} = \text{Im}[U_{xA}]$$

where $\varphi_x(\vec{k}_b, \mathbf{r}_x)$ describes x - A relative motion when b emerges with momentum $\vec{k}_b \equiv \{\Omega_b, E_b\}$. In the **Ichimura, Austern, Vincent (IAV)** DWBA model:

$$(E_x^+ - K_x - U_{xA}) \varphi_x^{\text{IAV}}(\mathbf{r}_x) = \langle \mathbf{r}_x \chi_b^{(-)} | V_{\text{post}} | \chi_a^{(+)} \phi_a \rangle$$

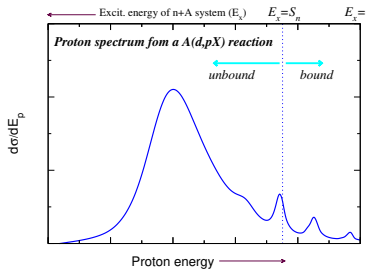
$$V_{\text{post}} \equiv V_{bx} + U_{bA} - U_{bB}$$

Interpretation of the U_{xA} potential

- For $E_x > 0$, U_{xA} is the usual optical model potential describing $x+A$ elastics
 - $\text{Im}[U_{xA}]$ accounts for $x - A$ **absorption**.
 - For $E_x < 0$, U_{xA} represents the distribution of single-particle (s.p.) states
 - $\text{Im}[U_{xA}]$ accounts for **s.p. fragmentation** (spreading widths).

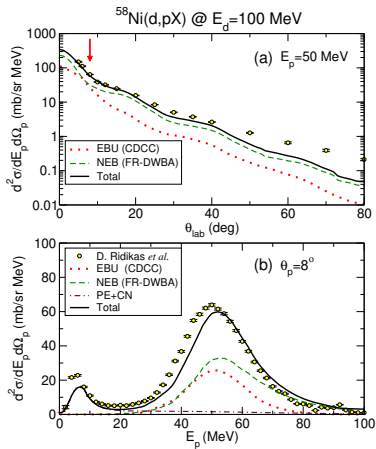
Interpretation of the U_{xA} potential

- ⇒ For $E_x > 0$, U_{xA} is the usual optical model potential describing $x+A$ elastics
 - ☞ $\text{Im}[U_{xA}]$ accounts for $x - A$ **absorption**.
 - ⇒ For $E_x < 0$, U_{xA} represents the distribution of single-particle (s.p.) states
 - ☞ $\text{Im}[U_{xA}]$ accounts for **s.p. fragmentation** (spreading widths).
-
- ⇒ These properties are naturally accommodated in *dispersive optical model (DOM)* potentials
 - ⇒ Both “transfer” to unbound states and bound states described on an equal footing



Comparison with inclusive breakup data

Application of IAV model to deuteron inclusive breakup



- ⇒ EBU calculated with CDCC.
- ⇒ NBU calculated with DWBA IAV model.
- ⇒ Low-energy protons from preequilibrium (PE) and compound nucleus (CN) evaporation not accounted for by IAV model, but can be evaluated with HF theory.

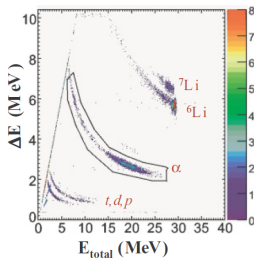
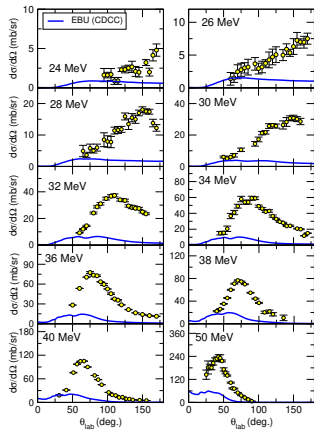
Data: Ridikas et al, PRC63, 014610 (2000)

Calc.: J. Lei, A.M.M., PRC 92, 044616 (2015); Jin Lei, Ph.D. thesis,
<https://idus.us.es/handle/11441/44344>



Application to ^{209}Bi ($^6\text{Li}, \alpha$)X

- ⇒ Large α yield ($\sigma_\alpha \gg \sigma_d$) ⇒ evidence of NEB channels
- ⇒ EBU alone cannot explain the data.

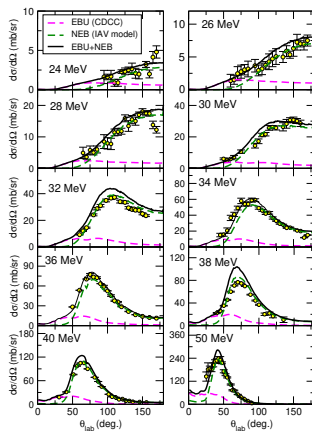




Application to ^{209}Bi ($^6\text{Li}, \alpha$)X

Assume: $\sigma_\alpha \simeq \sigma^{\text{EBU}} + \sigma^{\text{NEB}}$:

- ⇒ EBU ⇒ CDCC
- ⇒ NEB ⇒ IAV

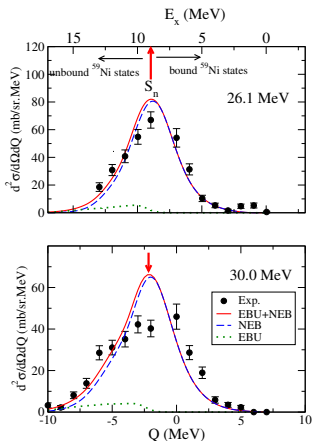
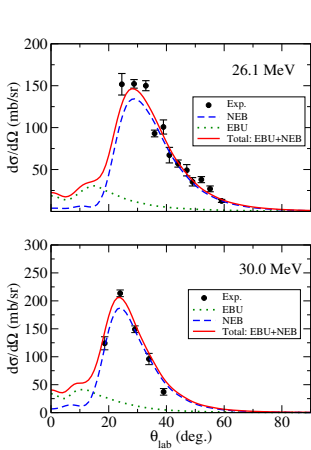


- ⇒ Inclusive data are well accounted for by EBU+NEB
- ⇒ Inclusive α 's dominated by NEB
- ⇒ EBU ($^6\text{Li} \rightarrow \alpha + d$) only relevant for small scattering angles.

Application to ^{58}Ni ($^8\text{Li}, ^7\text{Li}$)X

$${}^8\text{Li} \rightarrow {}^7\text{Li} ;$$

$^{58}\text{Ni}(^{8}\text{Li},^{7}\text{Li})\text{X}$ @ RIBRAS

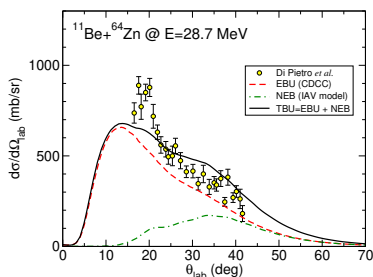


[O.C.B. Santos, PRC 103, 064601 (2021) and Ph.D. thesis]

Application to halo nuclei

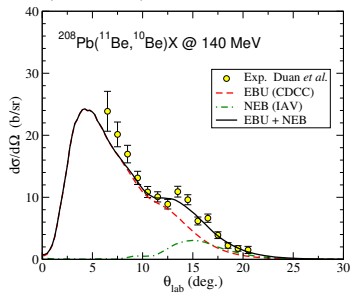
$$^{11}\text{Be} \rightarrow ^{10}\text{Be};$$

$^{64}\text{Zn}(\text{Be}^{11}, \text{Be}^{10})\text{X}$ @ ISOLDE-CERN



Di Pietro *et al.*, PLB 798 (2019) 134954

$^{208}\text{Pb}(\text{Be}, \text{X})$ @ HIRF-Lanzhou



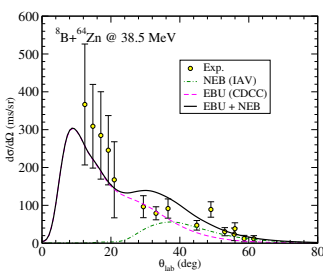
Duan *et al.*, PLB 811 (2020) 135942

- ⇒ Inclusive breakup dominated by EBU.
 - ⇒ NEB only important around the grazing angle.

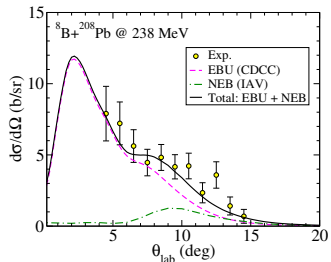
Application to halo nuclei

$${}^8\text{B} \rightarrow {}^7\text{Be};$$

$^{64}\text{Zn}(^{8}\text{B},^{7}\text{Be})\text{X}$ @ ISOLDE-CERN



$^{208}\text{Pb}(^{8}\text{B},^{7}\text{Be})\text{X}$ @ HIRF-Lanzhou



Wang et al, PRC 103, 024606 (2021)

Sparta et al, PLB820, 136477 (2021)

- ⇒ Inclusive breakup dominated by EBU.
 - ⇒ NEB important around the grazing angle.

Summary of inclusive breakup analyses

- ⇒ For weakly-bound, non-halo nuclei (deuteron, $^{6,7,8}\text{Li},..$) the inclusive breakup is dominated by the NEB component.
- ⇒ For very weakly-bound nuclei, such as halo nuclei ($^8\text{B},^{11}\text{Be}$), the inclusive breakup is dominated by the EBU component.
- ⇒ A significant part of the inclusive cross section corresponds to the population of continuum states of the residual ($x+A$) system.

Applications of the IAV model to fusion

Isolating the ICF part of NEB

- ⇒ NEB includes $x - A$ ICF, but also other nonelastic processes such as target excitation.
- ⇒ **Heuristic approach:** associate ICF with absorption inside the Coulomb barrier due to short-range imaginary potential W_{xA}^{fus} :

$$\frac{d\sigma^{\text{ICF}}}{d\Omega_b dE_b} \approx -\frac{2}{\hbar v_a} \rho_b(E_b) \langle \varphi_x | W_{xA}^{\text{fus}} | \varphi_x \rangle$$

Isolating the ICF part of NEB

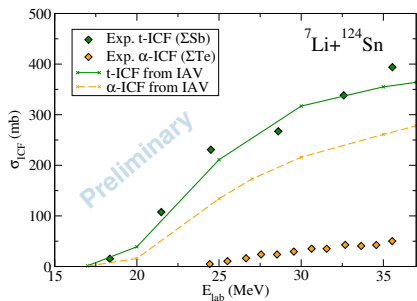
- ⇒ NEB includes $x - A$ ICF, but also other nonelastic processes such as target excitation.
- ⇒ **Heuristic approach:** associate ICF with absorption inside the Coulomb barrier due to short-range imaginary potential W_{xA}^{fus} :

$$\frac{d\sigma^{\text{ICF}}}{d\Omega_b dE_b} \approx -\frac{2}{\hbar v_a} \rho_b(E_b) \langle \varphi_x | W_{xA}^{\text{fus}} | \varphi_x \rangle$$

Caveats:

- ⇒ Energy dependence of W_{xA}^{fus} ?
- ⇒ Dependence of ICF on W_{xA}^{fus} parameters?
- ⇒ Presence of surface absorption in W_{AA} results in unphysically small ICF cross section

See alternative approaches by:

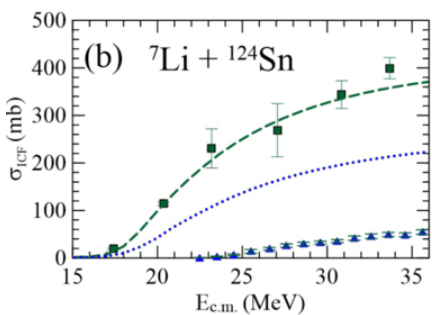
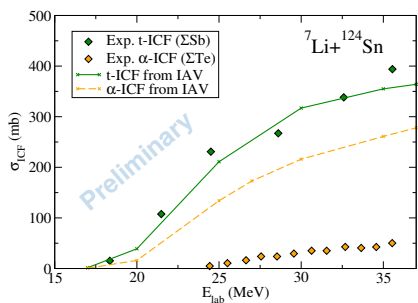
ICF in $^7\text{Li} + ^{124}\text{Sn}$ 

- ✓ t-ICF well reproduced
- ✗ ...but α -ICF largely overpredicted

Data: Parkar et al, PRC 97, 014607 (2018)



ICF in $^7\text{Li} + ^{124}\text{Sn}$

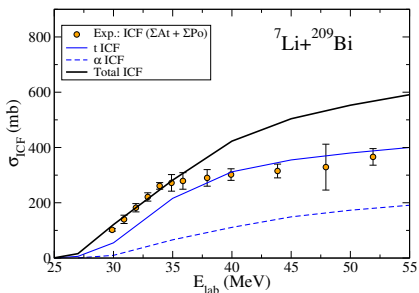


- ✓ t-ICF well reproduced
- ✗ ...but α-ICF largely overpredicted

Cortés et al, PRC102, 064628 (2021)

Data: Parkar et al, PRC 97, 014607 (2018)

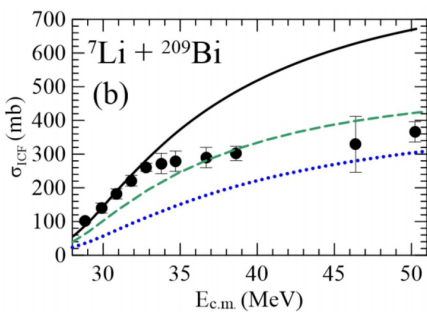
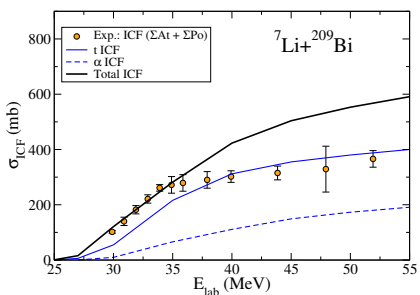
ICF in ${}^7\text{Li} + {}^{209}\text{Bi}$



- ✓ ICF well reproduced below $E_{\text{lab}} < 36$ MeV.
 - ✗ ...but overpredicted at higher incident energies

Data: Dasgupta et al, PRC 66, 041602(R) (2004); PRC 70, 024606 (2004)

ICF in $^7\text{Li} + ^{209}\text{Bi}$



- ✓ ICF well reproduced below $E_{\text{lab}} < 36 \text{ MeV}$.
- ✗ ...but overpredicted at higher incident energies

Cortés et al, PRC102, 064628 (2021)

Data: Dasgupta et al, PRC 66, 041602(R) (2004); PRC 70, 024606 (2004)

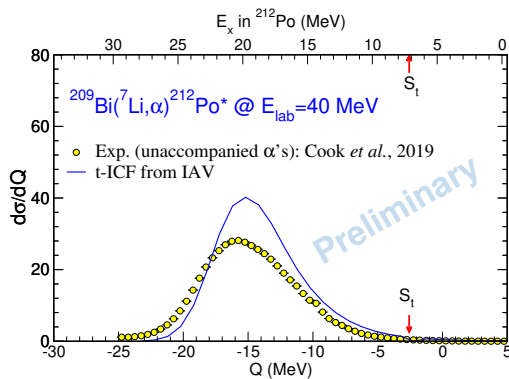


Excitation energy distribution of ICF in $^{7}\text{Li} + ^{209}\text{Bi}$

Since the theory provides the differential cross section,

$$\frac{d\sigma^{\text{ICF}}}{d\Omega_b dE_b}$$

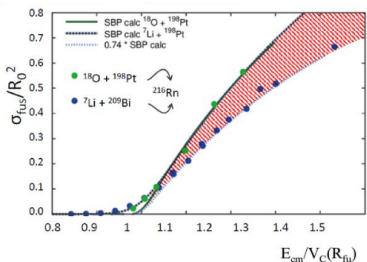
angular and energy distributions can also be obtained.



Data: Cook et al, PRL122, 102501 (2019)

The problem of complete fusion suppression at above-barrier energies

CF of weakly bound nuclei suppressed at energies above the Coulomb barrier:



- ⇒ Observed for weakly bound projectiles ($^{6,7,8}\text{Li}$, ^9Be)
 - ⇒ CF reduced by $\sim 30\%$ with respect to BPM or CC calculations.

M. Dasgupta et al., PRC 70, 024606 (2004)

Common interpretation:

- ⇒ CF is mostly reduced by **breakup** and **incomplete fusion (ICF)**.
 - ⇒ ICF is modeled as a **two-step** process: **elastic breakup** followed by **capture** of one charged fragment (breakup-fusion, BF).

Indirect evaluation of the CF cross section

- CF is related to other nonelastic channels by the **reaction cross section**.
For a two-body projectile ($a = b + x$):

$$\sigma_R \approx \sigma_{\text{CF}} + \sigma_{\text{inel}} + \sigma_{\text{EBU}} + \sigma_{\text{NEB}}^{(b)} + \sigma_{\text{NEB}}^{(x)}$$

- CF can be deduced from

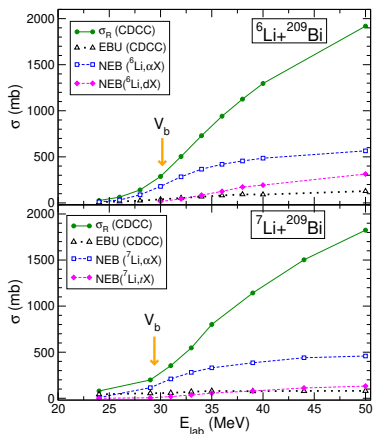
$$\sigma_{\text{CF}} \approx \underbrace{\sigma_R}_{\text{CDCC/OM}} - \underbrace{\sigma_{\text{inel}}}_{\text{CC/CDCC}} - \underbrace{\sigma_{\text{EBU}}}_{\text{CDCC}} - \underbrace{(\sigma_{\text{NEB}}^{(b)} + \sigma_{\text{NEB}}^{(x)})}_{\text{IAV model}}$$

N.b. Since ICF is part of the NEB, the calculated CF takes into account the flux going to ICF

Results for $^{6,7}\text{Li} + ^{209}\text{Bi}$

What is the relative contribution of the different nonelastic channels?

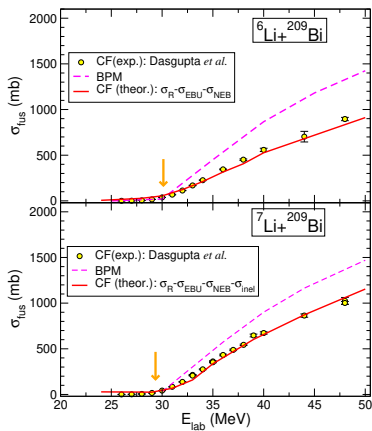
- ⇒ EBU: computed with CDCC
- ⇒ NEB: computed with IAV model



- ⇒ Dominant nonelastic channel is $^{209}\text{Bi}(^{6,7}\text{Li}, \alpha X)$
- ⇒ EBU ($\alpha + d$) mechanism gives a minor contribution to $\sigma_{\text{reac.}}$

Results for $^{6,7}\text{Li} + ^{209}\text{Bi}$

Effect of nonelastic channels on fusion



- ⇒ CF well reproduced
- ⇒ Suppression mostly due to NEB (eg. ICF)
- ⇒ Dominant channel reducing CF is $^{209}\text{Bi}(^{6,7}\text{Li}, \alpha)$
- ⇒ The EBU mechanism plays a minor role

Data: Dasgupta et al., PRC 70, 024606 (2004)

J. Lei, AMM, PRL122, 042503 (2019)